



GUIDANCE NOTES ON

**SPRINGING ASSESSMENT FOR CONTAINER CARRIERS
AND ORE CARRIERS**

JUNE 2017

**American Bureau of Shipping
Incorporated by Act of Legislature of
the State of New York 1862**

**© 2017 American Bureau of Shipping. All rights reserved.
ABS Plaza
16855 Northchase Drive
Houston, TX 77060 USA**

Foreword

The 2017 edition of these Guidance Notes expands the scope from just container carriers to include ore carriers; which has necessitated the title change to the *ABS Guidance Notes on Springing Assessment for Container Carriers and Ore Carriers*.

These Guidance Notes provide detailed procedures for the assessment of springing loads and the subsequent structural fatigue damage for container and ore carriers. The technical background is based on direct analysis of hydrodynamic load and structure dynamic response.

Additionally, these Guidance Notes supplement the Rules and Guides that ABS has issued for the Classification for container carriers. The *ABS Guide for Application of Higher-Strength Hull Structural Thick Steel Plates in Container Carriers* requires the evaluation of the springing effect on fatigue damage of hull structures. These Guidance Notes address how to carry out such evaluations.

The 2014 edition included an updated wave scatter diagram table and editorial changes.

The 2017 edition includes new and updated standard speed profiles, a new time-domain approach for fatigue damage, updated S-N curves to include second segment, and editorial changes.

These Guidance Notes become effective on the first day of the month of publication.

Users are advised to check periodically on the ABS website www.eagle.org to verify that this version of these Guidance Notes is the most current. Comments or suggestions can be sent electronically to rsd@eagle.org

Terms of Use

The information presented herein is intended solely to assist the reader in the methodologies and/or techniques discussed. These Guidance Notes do not and cannot replace the analysis and/or advice of a qualified professional. It is the responsibility of the reader to perform their own assessment and obtain professional advice. Information contained herein is considered to be pertinent at the time of publication, but may be invalidated as a result of subsequent legislations, regulations, standards, methods, and/or more updated information and the reader assumes full responsibility for compliance. This publication may not be copied or redistributed in part or in whole without prior written consent from ABS.



GUIDANCE NOTES ON

**SPRINGING ASSESSMENT FOR CONTAINER CARRIERS
AND ORE CARRIERS**

CONTENTS

SECTION 1	Introduction	1
1	General	1
2	Springing Phenomenon	1
3	Springing Assessment Procedure	2
	FIGURE 1 Time History of Measured Vertical Bending Moment	1
	FIGURE 2 Springing Assessment Procedure.....	3
SECTION 2	Loading Conditions, Speeds, and Headings	4
1	General	4
2	Loading Conditions	4
3	Standard Speed Profile.....	4
4	Wave Heading	4
	TABLE 1 Standard Speed Profile for Container Carriers.....	4
	TABLE 2 Standard Speed Profile for Ore Carriers.....	4
SECTION 3	Wave Environments.....	5
1	Wave Scatter Diagram.....	5
2	Wave Spectrum	5
	TABLE 1 ABS Wave Scatter Diagram for Unrestricted Service Classification.....	5
SECTION 4	Springing Susceptibility Assessment	7
1	General	7
2	Hull Girder Natural Frequency	7
3	Wave Characteristics	7
4	Springing Susceptibility.....	8
	FIGURE 1 Probability Distribution of T_z	8
	FIGURE 2 Typical Dynamic Amplification Factor.....	9
	FIGURE 3 Springing Susceptibility Indicator	9

SECTION 5	Calculation of Response Amplitude Operator	10
1	General	10
2	Vertical Bending Moment RAOs of Rigid Body.....	10
2.1	General Modeling Consideration	11
2.2	Hydrostatic Balance.....	11
2.3	Roll Damping	11
3	Vertical Bending Moment RAO of Flexible Body	12
3.1	Calculation of 2-Node Vibration Mode	12
3.2	Hydroelasticity	13
3.3	Large Range of Wave Frequency.....	13
4	Springing Damping	14
5	Stress RAO Calculation	14
FIGURE 1	Definition of Ship Motion	10
FIGURE 2	Vertical Bending Moment RAO (rigid body).....	12
FIGURE 3	2-Node Vertical Vibration Mode.....	12
FIGURE 4	Bending Stiffness Distribution	13
FIGURE 5	Vertical Bending RAO Distribution	13
SECTION 6	Response Statistics	15
1	General	15
2	Short Term Statistics.....	15
FIGURE 1	Vertical Bending Moment Response Spectra.....	16
SECTION 7	Fatigue Assessment.....	17
1	General	17
2	Frequency-Domain Approach for Fatigue Damage.....	17
2.1	General.....	17
2.2	Wave-Frequency Response Fatigue Damage	18
2.3	Combined Wave and Springing Response Fatigue Damage.....	18
3	Time-Domain Approach for Fatigue Damage	19
3.1	General.....	19
3.2	Short-Term Fatigue Damage	20
3.3	Long-Term Fatigue Damage.....	20
4	Fatigue Damage Assessment.....	21
4.1	Springing Contribution to Fatigue Damage.....	21
4.2	Fatigue Damage Assessment.....	21
APPENDIX 1	Fatigue Strength Assessment.....	22
1	General	22
1.1	Note.....	22
1.2	Applicability.....	22
1.3	Loadings	22
1.4	Effects of Corrosion	22
1.5	Format of the Criteria.....	22

2	Connections to be Considered for the Fatigue Strength Assessment	23
2.1	General.....	23
2.2	Guidance on Locations for Container Carriers	23
2.3	Guidance on Locations for Ore Carriers	23
2.4	Fatigue Classification	24
3	Fatigue Damage Calculation	36
3.1	Assumptions.....	36
3.2	Criteria.....	37
3.3	Long Term Stress Distribution Parameter, γ	37
3.4	Fatigue Damage.....	37
4	Fatigue Inducing Loads and Load Combination Cases.....	40
4.1	General.....	40
4.2	Wave-induced Loads.....	40
4.3	Combinations of Load Cases for Fatigue Assessment.....	40
5	Determination of Wave-induced Stress Range	41
5.1	General.....	41
5.2	Hatch Corners	41
6	Hot Spot Stress Approach with Finite Element Analysis	50
6.1	Introduction.....	50
6.2	Calculation of Hot Spot Stress at a Weld Toe	51
6.3	Calculation of Hot Spot Stress at the Edge of Cut-out or Bracket	53
TABLE 1	Fatigue Classification for Structural Details	25
TABLE 2	Welded Joint with Two or More Load Carrying Members for Container Carriers.....	28
TABLE 3	Welded Joint with Two or More Load Carrying Members for Ore Carriers	34
TABLE 4	Combined Load Cases for Fatigue Strength Formulation for Container Carriers.....	40
TABLE 5	Combined Load Cases for Fatigue Strength Formulation for Ore Carriers	41
FIGURE 1	Basic Design S-N Curves	39
FIGURE 2	Hatch Corners at Decks and Coaming Top	48
FIGURE 3	Circular Shape	49
FIGURE 4	Double Curvature Shape	49
FIGURE 5	Elliptical Shape.....	49
FIGURE 6	Hatch Corner for Longitudinal Deck Girder.....	50
FIGURE 7	51
FIGURE 8	53

This Page Intentionally Left Blank



SECTION 1 Introduction

1 General (1 June 2017)

The design and construction of the hull, superstructure, and deckhouses of container carriers **and ore carriers** are to be based on the applicable requirements of the ABS Rules and Guides. As a supplement to the ABS Rules and Guides, these Guidance Notes provide detailed procedures for assessment of springing and the subsequent structural fatigue damage for container carriers **and ore carriers**. The procedure is easy to use and can be utilized to make quick estimates of the fatigue damage due to springing at the conceptual design phase and to perform a sensitivity study of its variation with main dimensions and operational profiles. The technical background is based on the direct analysis of hydrodynamic load and structure dynamic response.

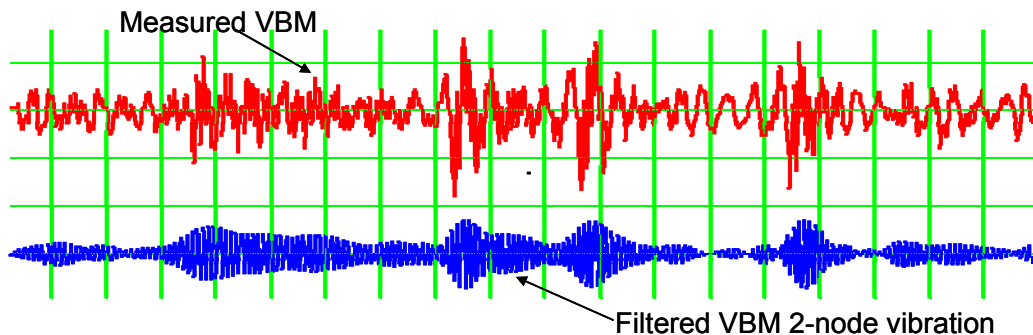
2 Springing Phenomenon (1 June 2017)

Springing is wave-induced hull girder vibration, and it is mainly excited by waves with an encounter frequency coinciding with the springing frequency. For a hull girder vibration, the most important springing frequency is its 2-node vertical natural vibration frequency. Springing can also be excited by waves with an encounter frequency of half of the springing frequency due to the second order contribution to the response. Springing could increase the fatigue load of the vessel, although its contribution to the extreme hull girder load may not be significant.

Springing is not a new topic. Early springing research has mainly focused on inland water ships. These ships, with large length/depth ratios, are flexible operating at low draft. Springing was not considered important for oceangoing ships due to the general observation that oceangoing vessels were relatively more rigid and their hull girder natural frequencies of vibration are farther away from the encountered wave frequencies.

However, wave-induced hull girder vibration has been observed from full-scale measurements in oceangoing ships (see Section 1, Figure 1). Also, with the rapid growth in ship size, especially container carriers, the new and next generations of post-Panamax container carriers are relatively flexible. These Guidance Notes provide procedures on the assessment of springing contribution to the structural fatigue damage and focus on the application to container carriers **and ore carriers**.

FIGURE 1
Time History of Measured Vertical Bending Moment



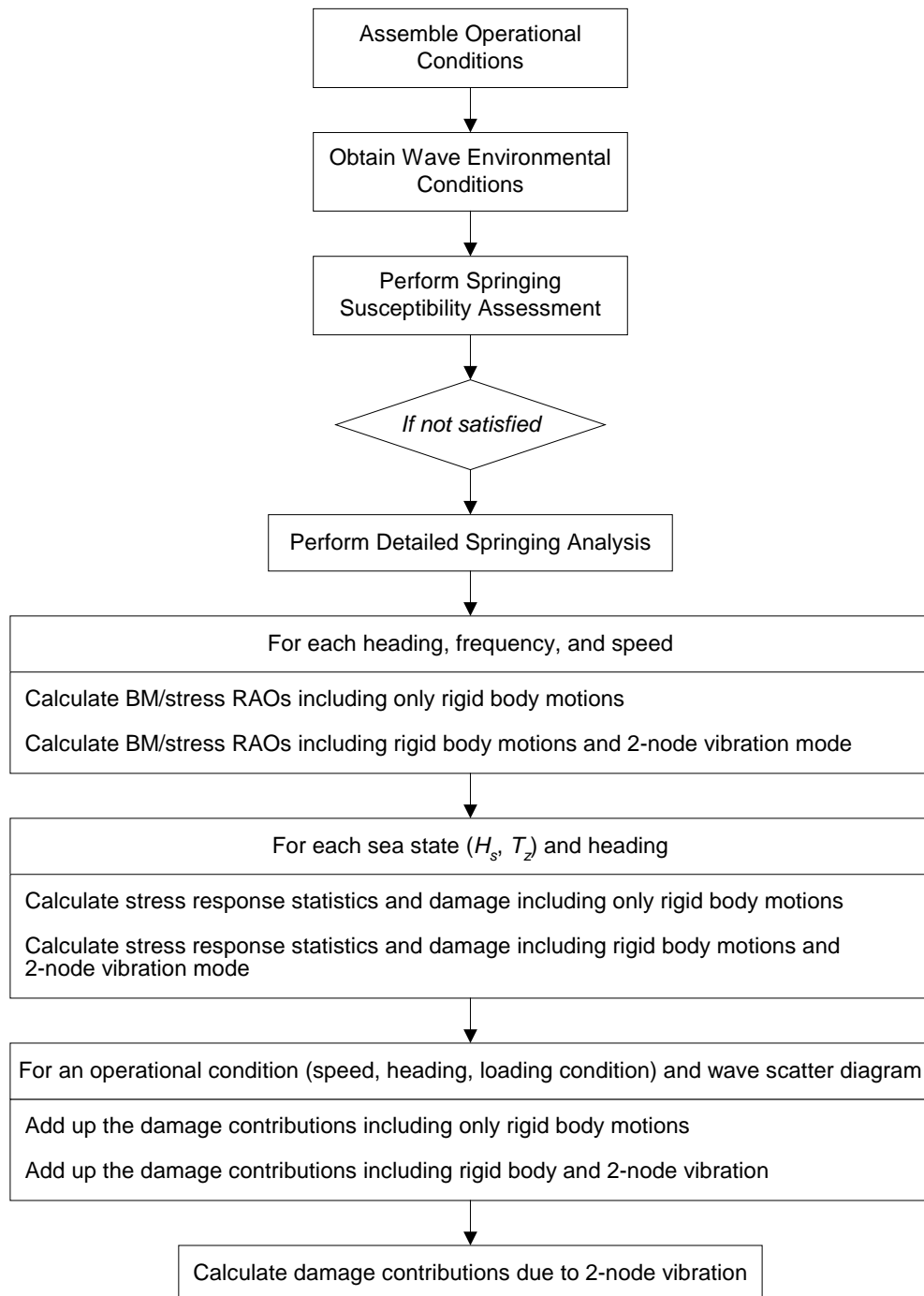
3 Springing Assessment Procedure

The recommended springing assessment procedure includes the following:

- i)* Determine the critical loading conditions, forward speed, and operational headings.
- ii)* Select wave environmental data, such as wave scatter diagram and wave spectrum.
- iii)* Perform springing susceptibility assessment.
- iv)* Perform detailed springing assessment:
 - Calculate vertical bending moment/stress RAOs including only rigid body motions.
 - Calculate vertical bending moment/stress RAOs including rigid body motions and 2-node vibration.
 - Calculate stress response statistics and fatigue damage including only rigid body motions.
 - Calculate stress response statistics and fatigue damage including rigid body motions and 2-node vibration.
 - Calculate total fatigue damage including only rigid body motions.
 - Calculate total fatigue damage including rigid body motions and 2-node vibration.
 - Calculate springing contribution to fatigue damage.

The analysis flowchart is given in Section 1, Figure 2. Detailed descriptions for the analysis procedures are given in Sections 2 through 7.

FIGURE 2
Springing Assessment Procedure





SECTION 2 Loading Conditions, Speeds, and Headings

1 General

For a given vessel, springing is influenced by, among other factors, loading conditions, encountered waves, and vessel speed. These conditions need to be considered in the springing assessment.

2 Loading Conditions (1 June 2017)

For the fatigue assessment of a vessel, a minimum of two loading conditions is recommended:

- Homogeneous loading condition at design draft
- Homogeneous loading condition at lowest draft

3 Standard Speed Profile (1 June 2017)

In high seas, the ship speed may be reduced voluntarily or involuntarily. If a specific operational profile for the vessel is not available, a standard speed profile is to be applied based on the significant wave height as shown in Section 2, Table 1 for container carriers and Section 2, Table 2 for ore carriers, where V_d is the design speed.

4 Wave Heading

It is assumed that springing mainly occurs in bow sea conditions. It is recommended that wave headings of head sea (180-degree), 165-degree, and 150-degree bow seas are to be included in the springing analysis.

TABLE 1
Standard Speed Profile for Container Carriers (1 June 2017)

<i>Significant Wave Height, H_s</i>	<i>Speed</i>
$0 < H_s \leq 6.0 \text{ m (19.7 ft)}$	100% V_d
$6.0 \text{ m (19.7 ft)} < H_s \leq 9.0 \text{ m (29.5 ft)}$	75% V_d
$9.0 \text{ m (29.5 ft)} < H_s \leq 12.0 \text{ m (39.4 ft)}$	50% V_d
$12.0 \text{ m (39.4 ft)} < H_s$	25% V_d

TABLE 2
Standard Speed Profile for Ore Carriers (1 June 2017)

<i>Significant Wave Height, H_s</i>	<i>Speed</i>
$0 < H_s \leq 4.0 \text{ m (13.1 ft)}$	100% V_d
$4.0 \text{ m (13.1 ft)} < H_s \leq 6.0 \text{ m (19.7 ft)}$	75% V_d
$6.0 \text{ m (19.7 ft)} < H_s \leq 9.0 \text{ m (29.5 ft)}$	50% V_d
$9.0 \text{ m (29.5 ft)} < H_s$	25% V_d



SECTION 3 Wave Environments

1 Wave Scatter Diagram (1 February 2014)

As seagoing vessels are typically designed for unrestricted service in the North Atlantic, the wave scatter diagram given in Section 3, Table 1. The numbers in the diagram represent the probability of sea states described as occurrences per 100,000 observations.

TABLE 1
ABS Wave Scatter Diagram for Unrestricted Service Classification (1 February 2014)

* Wave heights taken as significant values, H_s

** Wave periods taken as zero crossing values, T_z

		Wave Period (sec)**											Sum Over All Periods	
		3.50	4.50	5.50	6.50	7.50	8.50	9.50	10.50	11.50	12.50	13.50		
Wave Height (m)*	0.5	8	260	1344	2149	1349	413	76	10	1			5610	
	1.5		55	1223	5349	7569	4788	1698	397	69	9	1	21158	
	2.5		9	406	3245	7844	7977	4305	1458	351	65	10	25670	
	3.5			2	113	1332	4599	6488	4716	2092	642	149	28	20161
	4.5				30	469	2101	3779	3439	1876	696	192	43	12625
	5.5				8	156	858	1867	2030	1307	564	180	46	7016
	6.5				2	52	336	856	1077	795	390	140	40	3688
	7.5				1	18	132	383	545	452	247	98	30	1906
	8.5					6	53	172	272	250	150	65	22	990
	9.5					2	22	78	136	137	90	42	15	522
	10.5					1	9	37	70	76	53	26	10	282
	11.5						4	18	36	42	32	17	7	156
	12.5						2	9	19	24	19	11	4	88
	13.5						1	4	10	14	12	7	3	51
>14.5						1	5	13	19	19	13	7	77	
Sum over All Heights		8	326	3127	12779	24880	26874	18442	8949	3335	1014	266	100000	

2 Wave Spectrum

Sea wave conditions are to be modeled by the two-parameter Bretschneider spectrum, which is determined by the significant wave height and the zero-crossing wave period of a sea state. The wave spectrum is given by:

$$S_{\zeta}(\omega) = \frac{5\omega_p^4 H_s^2}{16\omega^5} \exp\left[-1.25(\omega_p / \omega)^4\right]$$

where

- S_{ζ} = wave energy density, m²-sec (ft²-sec)
- H_s = significant wave height, m (ft)
- ω = angular frequency of wave component, rad/sec
- ω_p = peak frequency, rad/sec
- = $2\pi/T_p$
- T_p = peak period, sec
- = $1.408 T_z$

To consider short-crested waves, “cosine squared” spreading is to be utilized, which is defined as:

$$f(\beta) = k \cos^2(\beta - \beta_0)$$

where

- β = wave heading, following sea is 0 degrees, and head sea is 180 degrees, in the range of

$$\beta_0 - \frac{\pi}{2} \leq \beta \leq \beta_0 + \frac{\pi}{2}$$
- β_0 = main wave heading of a short-crested wave
- k = factor determined such that the summation of $f(\beta)$ is equal to 1.0, i.e.:

$$= \sum_{\beta_0 - \pi/2}^{\beta_0 + \pi/2} f(\beta) = 1$$



SECTION 4 Springing Susceptibility Assessment

1 General

Springing is wave-induced vibration. Its effect on the operation and the structure of vessels can become important when the natural frequency of the vessel is close to the encountered wave frequency. If the natural frequency of the vessel is far from that of encountered waves, springing effect may be considered as insignificant. The first step in the springing assessment is to evaluate the springing susceptibility of the vessel. This Section describes the recommended springing susceptibility criteria.

2 Hull Girder Natural Frequency (1 February 2014)

The hull girder natural frequency can be obtained through finite element method, beam method, or full-scale measurement. If they are not available, the following formula can be used to estimate hull girder natural frequency:

$$\omega_n = \mu [I_v / (\Delta_i L_{BP}^3)]^{1/2}, \text{ rad/sec}$$

where:

μ	=	321500 (176118)
I_v	=	moment of inertia, m ⁴ (ft ⁴)
Δ_i	=	virtual displacement, including added mass of water, t (Lt)
	=	$[1.2 + B/(3d_m)] \Delta$
B	=	breadth of vessel, m (ft)
d_m	=	mean draft of vessel, m (ft)
Δ	=	vessel displacement, t (Lt)
L_{BP}	=	vessel's length between perpendiculars, m (ft)

3 Wave Characteristics (1 June 2017)

Waves are normally generated by winds and they are random in nature. Waves can be characterized by zero up-crossing periods, peak periods, wave energy spectrum, and other parameters. For a sea state (or storm), the peak period is defined as the wave period at which the wave energy spectrum reaches its peak. It means that the greatest wave energy of the storm is associated with that wave period.

For a fully developed sea, the relationship of peak period and zero up-crossing period can be written as:

$$T_p = 1.408 T_z \text{ sec}$$

where T_p is peak period and T_z is zero up-crossing period in second.

The peak frequency is the inverse of the peak period. The vessel encountered wave frequency can be written as:

$$\omega_e = \omega - \omega^2 V/g \cos(\beta) \text{ rad/sec}$$

where

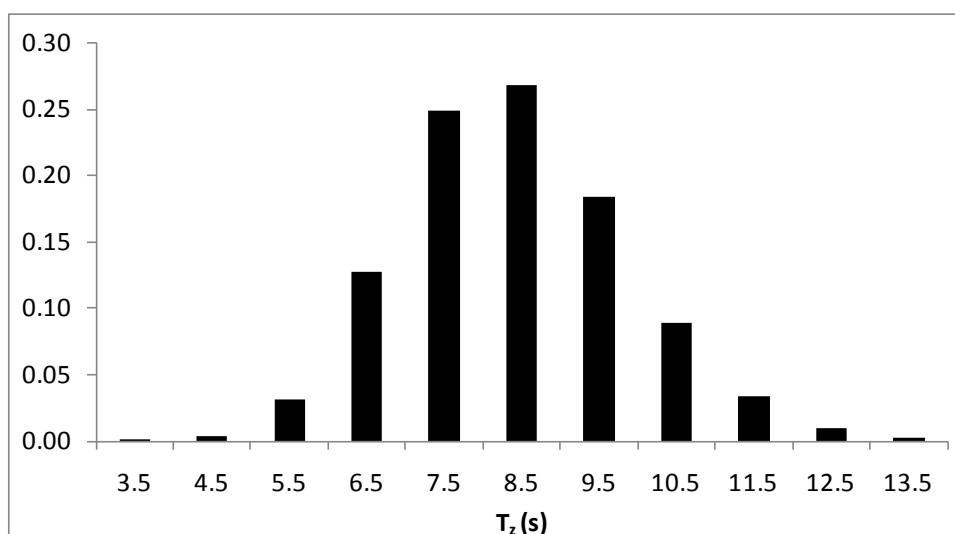
- ω = wave frequency, rad/sec
- V = vessel forward speed, m/sec (ft/sec)
- g = acceleration of gravity, m/sec² (ft/sec²)
- β = wave heading

For head sea conditions, the **encountered** frequency can be written as:

$$\omega_e = \frac{2\pi}{T_p} + \left(\frac{2\pi}{T_p}\right)^2 V/g \text{ rad/sec}$$

For North Atlantic waves, Section 4, Figure 1 depicts the probability distribution of zero crossing wave periods according to Section 3, Table 1.

FIGURE 1
Probability Distribution of T_z (1 February 2014)



4 Springing Susceptibility (1 June 2017)

Springing is a dynamic response of the hull girder to the wave load. As for any dynamic problem, the dynamic response amplification factor can range from near zero to a very high value at the resonance frequency. Section 4, Figure 2 depicts the dynamic amplification factor for a typical one-degree-of-freedom vibration problem. The x-axis in the plot is the ratio of load frequency to the natural frequency of the system.

To avoid a large dynamic response, the system should be designed so that the natural frequency of the system is far from the load frequency.

For a **vessel**, the springing susceptibility indicator can be formulated based on the natural frequency of the 2-node hull girder vibration and the **encountered** wave frequency. If the natural frequency of the 2-node vibration mode is greater than approximately three times that of the **encountered** wave frequency, springing is considered to be insignificant. According to Subsections 4/2 and 4/3, the springing susceptibility indicator, η , can be written as:

$$\eta = 3 \frac{\omega_e}{\omega_n}$$

If the indicator is larger than one, a further detailed springing analysis is recommended. Section 4, Figure 3 shows an example plot for η as a function of ship speed and wave period. Typically, the **short** waves that are usually associated with the **shorter** wave periods are **more** important for springing.

FIGURE 2
Typical Dynamic Amplification Factor

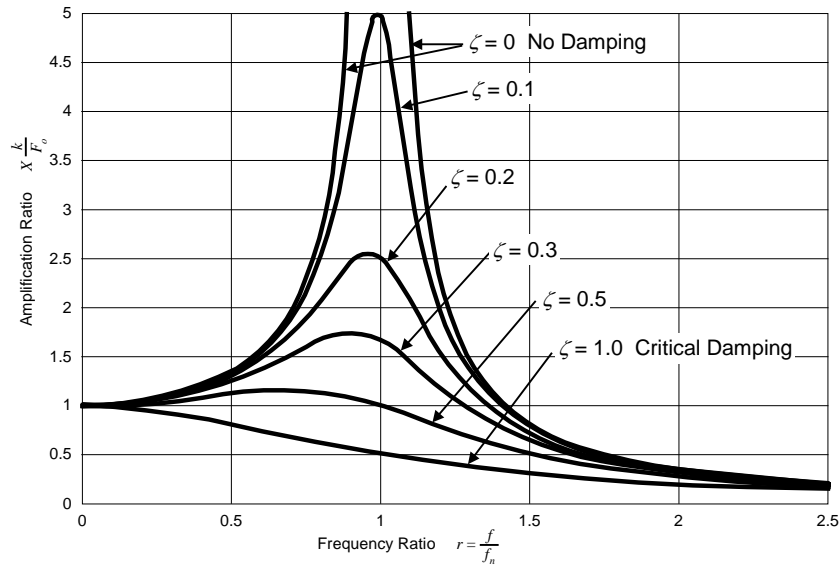
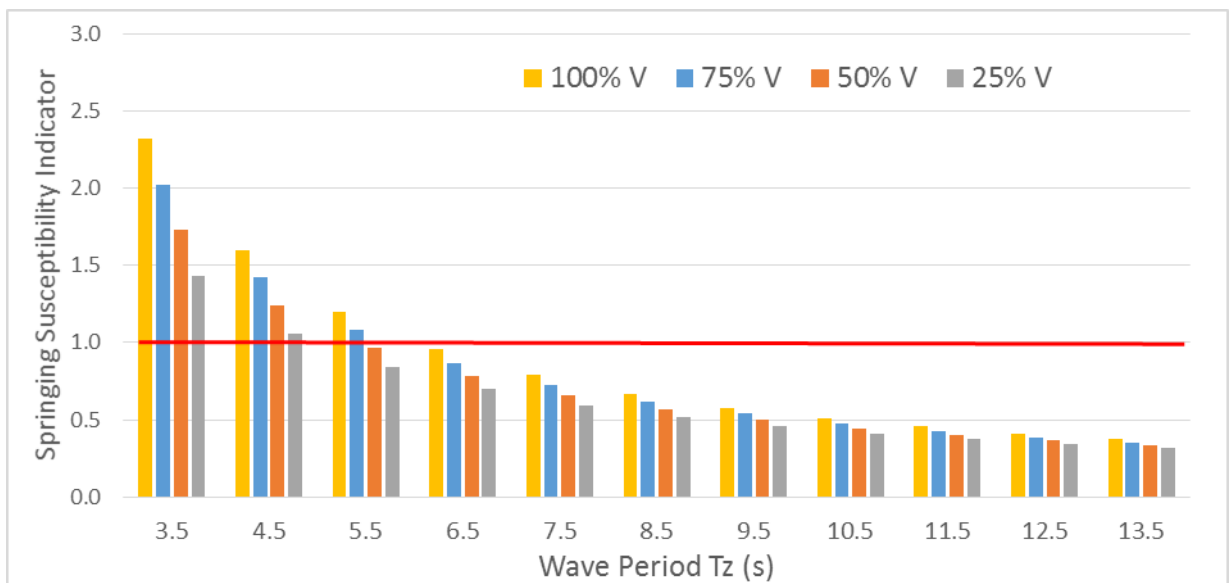


FIGURE 3
Springing Susceptibility Indicator (1 June 2017)



SECTION 5 Calculation of Response Amplitude Operator

1 General

Springing mainly increases hull girder fatigue load. The detailed springing analysis includes the calculation of response amplitude operator (RAO) of vertical bending moment, the response statistics and the fatigue damage calculation. The objective of the detailed springing analysis is to obtain the springing contribution to the fatigue damage of the vessel structure. The contribution can be defined as the ratio of the fatigue damage due to springing to that when vessel is considered as rigid body.

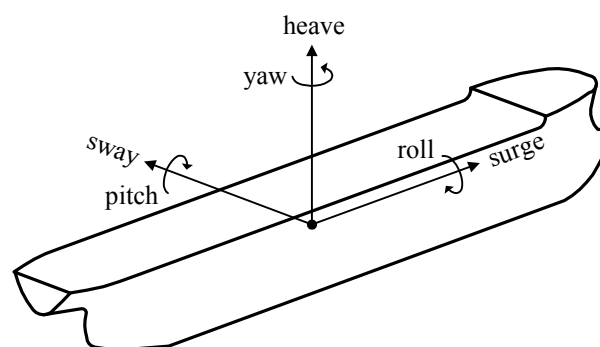
Springing can be excited when the encountered wave frequency is close to the natural frequency of the hull girder 2-node vibration mode. It can also be excited when the encountered wave frequency is about the half of the 2-node vibration frequency due to second order wave effects. Therefore, the second order seakeeping analysis approach may be used for the calculation of vertical bending moment.

This Section provides procedures for the calculation of bending moment RAOs of vessels with springing (flexible vessels) and without springing (rigid vessels).

2 Vertical Bending Moment RAOs of Rigid Body

The Response Amplitude Operators (RAOs) are the vessel's responses to unit amplitude, regular, sinusoidal waves. The vertical bending moment RAOs of a rigid body can be obtained through a conventional seakeeping analysis in which six degrees of rigid body motions are included in the analysis. The six degrees of motion are surge, sway, heave, roll, pitch, and yaw. Section 5, Figure 1 illustrates the definition of six degrees of motion.

FIGURE 1
Definition of Ship Motion



A frequency domain analysis program, in general, can be used for the calculation of the RAOs. Two-dimensional strip theory and three-dimension panel method are also applicable for the calculation of RAOs.

A sufficient range of wave headings and frequencies should be considered for the calculation of RAOs. The Response Amplitude Operators are to be calculated for wave headings from head seas (180 degrees) to following seas (0 degrees) in increments of 15 degrees. It is recommended that the range of wave frequencies include 0.2 rad/s to 2.0 rad/s in increments of 0.05 rad/s.

2.1 General Modeling Consideration

For each loading condition, the draft at F.P. and A.P., the location of center of gravity, radii of gyration, and sectional mass distribution along the ship length are to be prepared from the Trim and Stability booklet. The free surface GM correction is to be considered for partially filled tanks. For a tank with filling level above 98% or below 2% of the tank height, the free surface GM correction may be ignored.

The evaluation of the seakeeping analysis model should include the following:

2.2 Hydrostatic Balance

For each cargo loading condition, the hydrostatics of the vessel calculated based on the panel model are to be verified. At a statically balanced loading condition, the displacement, trim and draft, Longitudinal Center of Buoyancy (LCB), transverse metacentric height (GMT), and longitudinal metacentric height (GML) should be checked against the values provided in the trim and stability booklet. The differences should be within the following tolerances:

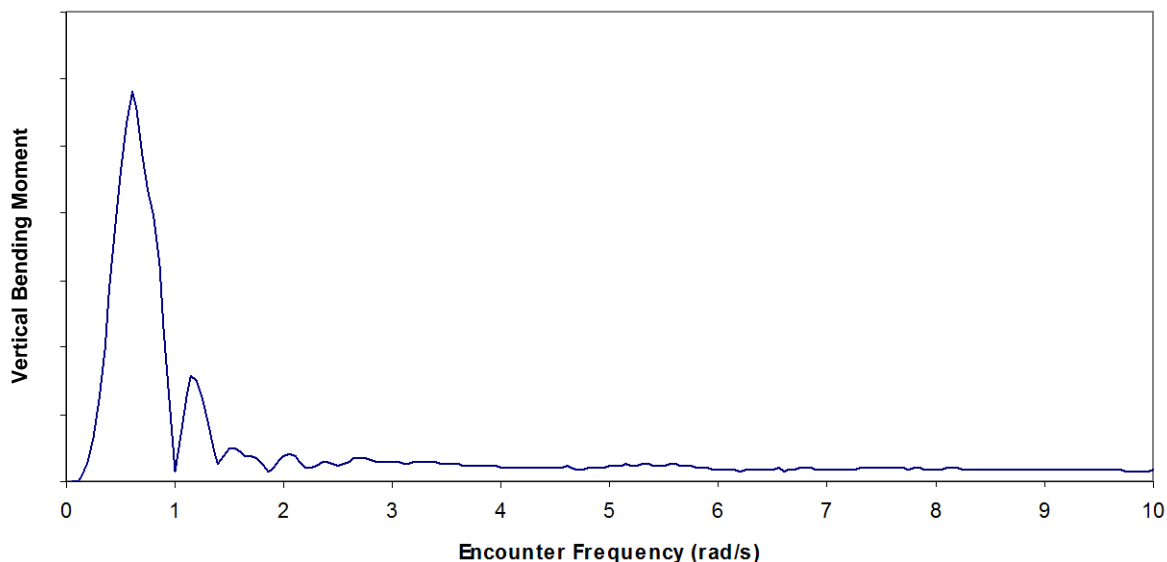
Displacement:	$\pm 1\%$
Trim:	± 0.1 degrees
Draft:	
Forward	± 1 cm (0.4 in.)
Aft	± 1 cm (0.4 in.)
LCB:	$\pm 0.1\%$ of length
GMT:	$\pm 2\%$
GML:	$\pm 2\%$
SWBM:	$\pm 5\%$

2.3 Roll Damping

The roll motion of a vessel at beam or oblique seas is greatly affected by viscous roll damping, especially with wave frequencies near the roll resonance frequency. For seakeeping analysis based on potential flow theory, a proper viscous roll damping model is required. Experimental data or empirical methods can be used for the determination of the viscous roll damping. In addition to the hull viscous damping, the roll damping due to rudders and bilge keels is to be considered. If this information is not available, 10% of critical damping may be used for overall viscous roll damping.

Section 5, Figure 2 is a typical vertical bending moment RAO plot including second order wave effect.

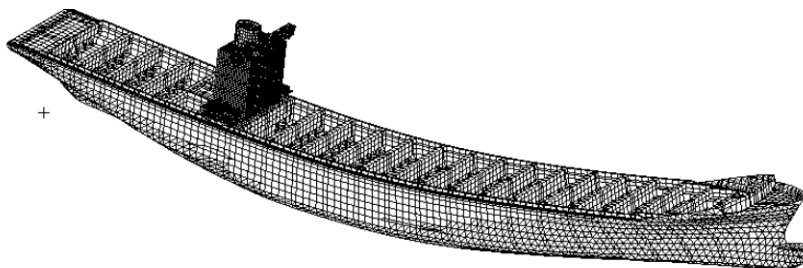
FIGURE 2
Vertical Bending Moment RAO (rigid body)



3 Vertical Bending Moment RAO of Flexible Body

The calculation of the vertical bending moment RAO of a flexible body is similar to that for a rigid body but with the extension to the flexible mode of motion (i.e., 2-node hull girder vibration mode). Section 5, Figure 3 is a plot of the 2-node vertical vibration mode of a container carrier.

FIGURE 3
2-Node Vertical Vibration Mode



For the vertical bending moment calculation of a flexible body, the following additional calculations are to be included in the analysis.

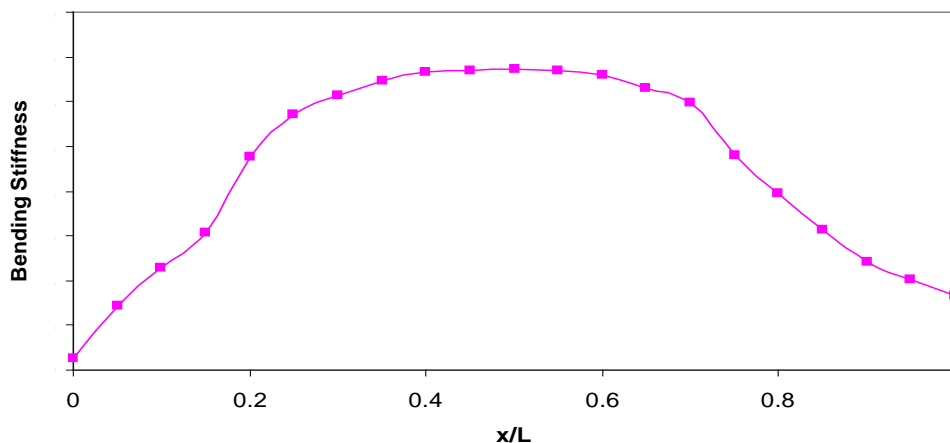
3.1 Calculation of 2-Node Vibration Mode

The 2-node vibration mode can be calculated using a finite element 3-D model or using a simplified one-dimensional non-uniform beam model. For the beam model, the vessel can be divided into a number of sections (21 or above). For each section, the following structural properties are to be provided:

- Mass per unit length
- Shear stiffness
- Bending stiffness
- Mass moment of inertia

Care is to be taken regarding the bending stiffness. Bending stiffness should include only the longitudinal continuous members and the changes in the bending stiffness should be avoided. Section 5, Figure 4 is a plot of the bending stiffness distribution along the vessel's length for a typical container carrier.

FIGURE 4
Bending Stiffness Distribution



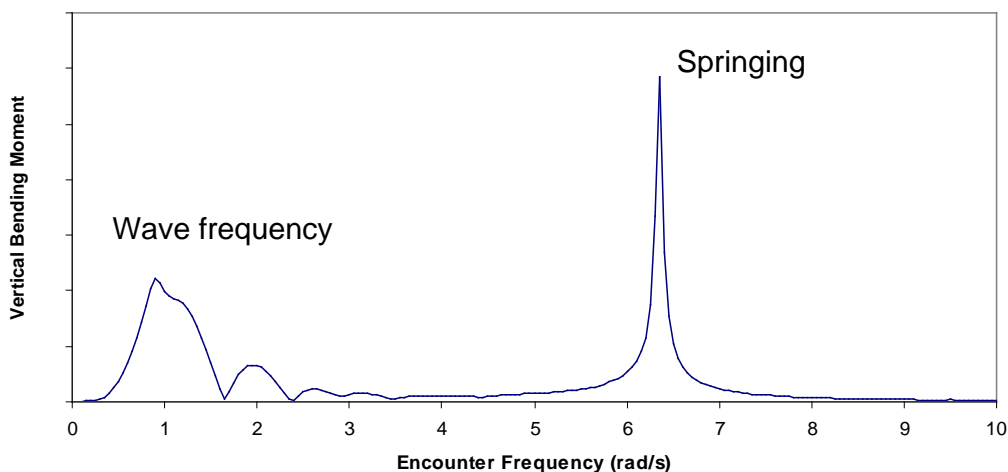
3.2 Hydroelasticity

The interaction of the 2-node vibration mode with the wave field is to be included in the seakeeping analysis. The interaction can be calculated through the generalized added mass and damping for the 2-node vibration mode. Two- or three-dimensional hydroelasticity programs can be used to account for the interaction.

3.3 Large Range of Wave Frequency

Extend the wave frequency range to cover the vibration response at its natural frequency, normally from 0.2 rad/s to 10 rad/s. Section 5, Figure 5 is a plot of vertical bending moment RAOs including springing for the head sea case.

FIGURE 5
Vertical Bending RAO Distribution



4 Springing Damping

Springing, in general, is a resonance phenomenon since wave excitation at the springing frequency is relatively small. Damping plays a very important role in the springing response. The total damping includes the structural damping, cargo damping, hydrodynamic damping, etc. The hydrodynamic damping can be evaluated through numerical analysis. Unfortunately, the actual magnitudes of structural and cargo damping are not easy to obtain. 1.5% to 3.0% of the critical damping may be used for ballast and full load conditions, respectively.

5 Stress RAO Calculation

Full-ship finite element analysis for stress calculation is not included in these Guidance Notes. The focus here is the springing contribution to the fatigue damage calculation. It is assumed that springing is mainly from the 2-node vertical vibration mode and the stress response can be represented by applying beam theory.

The stress RAOs can then be obtained through a stress influence coefficient, as shown below:

$$Stress(\omega, \beta) = VBM(\omega, \beta)/k$$

where

k = stress influence factor which can be approximated by the section modulus at the location along the vessel

ω = wave frequency, rad/sec

β = vessel's heading

$VBM(\omega, \beta)$ = vertical bending moment RAO

The same stress influence factor should be used for the stress RAOs of the rigid body only and for that of rigid body motion plus 2-node vibration motion.



SECTION 6 Response Statistics

1 General

In this Section, a method for statistical analysis of stress response is presented. The objective is to obtain the statistical characteristics of the stress response that will be used for the fatigue damage calculation.

2 Short Term Statistics

For each sea state, a spectral density function, $S_M(\omega, \beta)$, of the response under consideration at wave heading, β , may be calculated, within the scope of the linear theory, from the following equation:

$$S_M(\omega, \beta) = S_w(\omega) |H(\omega, \beta)|^2$$

where $S_w(\omega)$ represents the wave spectrum and $H(\omega, \beta)$ represents the Response Amplitude Operator (RAOs) at wave heading, β , as a function of the wave frequency denoted by ω . For a vessel with constant forward speed U , the n -th order spectral moment of the response at wave heading, β_0 , may be expressed by the following equation:

$$m_n = \sum_{\beta_0 - \pi/2}^{\beta_0 + \pi/2} \left[\int_0^{\infty} f(\beta) \omega_e^n S_y(\omega, \beta_0) d\omega \right]$$

where f represents the spreading function defined in Subsection 3/2, and ω_e represents the wave frequency of encounter defined by:

$$\omega_e = \left| \omega - U \frac{\omega^2}{g} \cos \beta \right|, \text{ rad/s}$$

where

- g = gravitational acceleration, m/s² (ft/s²)
- β = wave heading, following sea is 0 degrees, and head sea is 180 degrees, in the range of $\beta_0 - \frac{\pi}{2} \leq \beta \leq \beta_0 + \frac{\pi}{2}$
- β_0 = main wave heading angle of a short-crested wave

The standard deviation is the 0-th order of the response spectral moment.

For the second order method, the response spectra are obtained from three components. The first component is the usual linear response spectrum. The other two components are the second order components: slowly varying terms that are associated with the difference in frequencies ($\omega_r - \omega_s$) and rapidly varying terms that are associated with the sum of the frequencies ($\omega_r + \omega_s$). The response spectra for slowly and rapidly varying terms can be written, respectively, as:

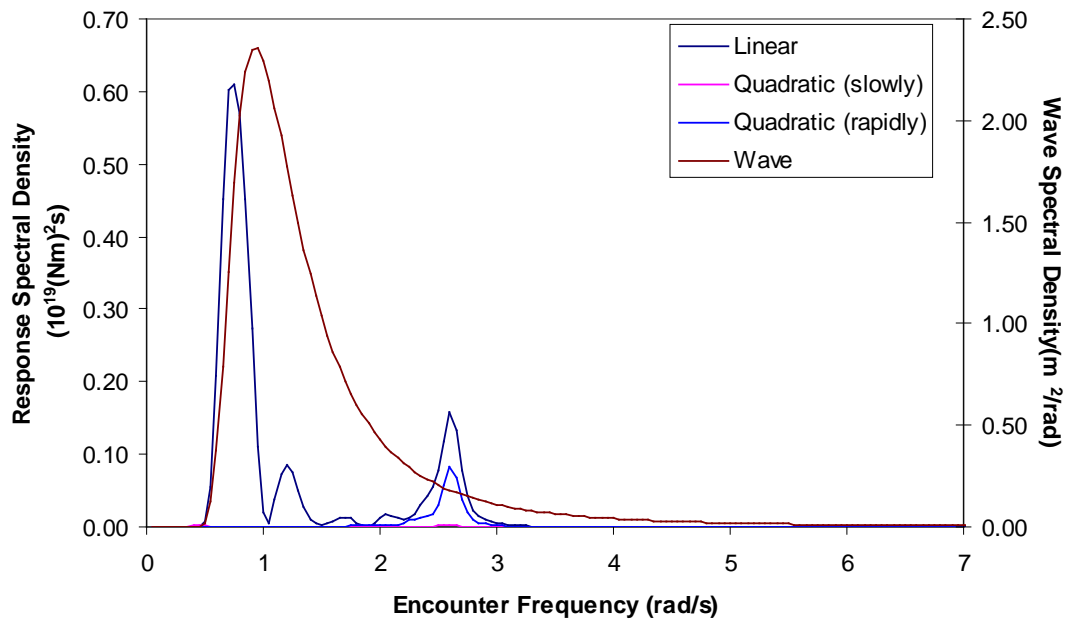
$$S_{M(2)}^-(\omega_r, \beta) = \sum_{\substack{t=1 \\ s=r+t}}^{n-r} 8 | (H_{st(2)}^-)^2 | S(\omega_s) S(\omega_t) \Delta\omega$$

$$S_{M(2)}^+(\omega_r, \beta) = \sum_{\substack{t=\max(1, r-n) \\ s=r-t}}^{\min(n, r-1)} 8 | (H_{st(2)}^+)^2 | S(\omega_s) S(\omega_t) \Delta\omega$$

Where $\omega_i = i\Delta\omega$, and H^- and H^+ are the transfer function for slowly and rapidly varying terms.

Section 6, Figure 1 is a plot of a normalized stress response spectra for a given sea state and a head sea case.

FIGURE 1
Vertical Bending Moment Response Spectra
 Hs=6(m), Tz=8(s), Speed=25(knots), Wave Ship Heading=180





SECTION 7 Fatigue Assessment

1 General (1 June 2017)

This Section provides procedures for the fatigue assessment of **vessels** including springing. It is assumed that the damage is mainly due to vertical bending moment. It is also assumed that springing occurs mainly in a bow seas wave environment.

The main objective of the assessment is to obtain the springing contribution to the fatigue damage relative to that from normal wave loads. The contribution as a factor of wave-induced damage can be used in the detailed fatigue assessment, such as in the *ABS Guide for Application of Higher-Strength Hull Structural Thick Steel Plates in Container Carriers* and others that are applicable.

The fatigue damage assessment, in general, includes the following three major steps:

- Prediction of fatigue damage without springing
- Prediction of fatigue damage including springing
- Springing contribution to the fatigue damage

2 Frequency-Domain Approach for Fatigue Damage (1 June 2017)

2.1 General (1 February 2014)

For a single one-segment linear S-N curve, the closed form expression of damage, D can be calculated as follows:

$$D = \frac{T}{K} (2\sqrt{2})^m \Gamma\left(\frac{m}{2} + 1\right) \sum_i \lambda(m, \varepsilon_i) f_{0i} p_i (\sigma_i)^m$$

where

- | | | |
|-----------------|---|------------------------------------------------------------------------------------|
| T | = | total target fatigue life, in seconds |
| K, m | = | physical parameters describing the S-N curve, as defined in Appendix 1, Figure 1 |
| Γ | = | complete gamma function |
| f_{0i} | = | zero up-crossing frequency of the stress amplitude at the i -th sea state, rad/s |
| p_i | = | probability of the i -th sea state in the wave scatter diagram |
| λ | = | wide-band correction factor, as defined below |
| σ_i | = | standard deviation of the stress amplitude at the i -th sea state |
| ε_i | = | spectral bandwidth, as defined below |

This formula for the damage calculation is mainly based on the narrow banded Gaussian process and Palmgren-Miner rule. For a wide-banded stress process, a correction factor may be introduced for the damage calculation. The following two Paragraphs provide the correction factors for wave frequency response and combined wave frequency and high frequency (springing) response.

2.2 Wave-Frequency Response Fatigue Damage

The zero up-crossing frequency of the stress due to wave frequency loads can be calculated by:

$$f_0 = \frac{1}{2\pi} \frac{\sigma_2}{\sigma_0}$$

where σ_0 and σ_2 are the zero and second spectral moment of the stress response, respectively, and can be written as:

$$\sigma_n^2 = \int_0^{\infty} \omega^n S(\omega) d\omega$$

where $S(\omega)$ is the stress spectral distribution function.

The wide-band correction factor can be calculated by:

$$\lambda(m, \varepsilon_i) = a(m) + [1 - a(m)][1 - \varepsilon_i]^{b(m)}$$

where

$$a(m) = 0.926 - 0.033m$$

$$b(m) = 1.587m - 2.323$$

$$\varepsilon = \sqrt{1 - \frac{\sigma_2^4}{\sigma_0^2 \sigma_4^2}}$$

2.3 Combined Wave and Springing Response Fatigue Damage

The hull girder response including springing is a wide-banded process. It includes normal wave response and high-frequency response components. The high frequency is normally about the 2-nodal hull girder vibration frequency.

The response can be separated into two narrow banded processes: wave-frequency and high-frequency response. The response statistics, such as the standard deviation of the response, for the two separated processes can be calculated independently as:

$$\sigma_{wave-n}^2 = \int_0^{\omega_1} \omega^n S(\omega) d\omega$$

$$\sigma_{springing-n}^2 = \int_{\omega_1}^{\infty} \omega^n S(\omega) d\omega$$

where ω_1 is the frequency at which the wave frequency response and springing are separated. It can be taken as 2.0 for a typical container carrier.

The zero up-crossing frequency for wave component stress and springing stress can be calculated as:

$$f_{wave} = \frac{1}{2\pi} \frac{\sigma_{wave-2}}{\sigma_{wave-0}}$$

$$f_{springing} = \frac{1}{2\pi} \frac{\sigma_{springing-2}}{\sigma_{springing-0}}$$

The total fatigue damage due to the wide-banded response to normal wave load and springing can be evaluated through the combined stress standard deviation and zero up-crossing frequency, and a stress cycle correction factor. They can be calculated using the following equations:

$$\sigma_I = \left(\sigma_{springing-0}^2 + \sigma_{wave-0}^2 \right)^{1/2}$$

$$f_{0i} = \left(f_{springing}^2 \sigma_{springing-0}^2 + f_{wavw}^2 \sigma_{wave-0}^2 \right)^{1/2} / \sigma_i$$

The stress cycle correction factor $\lambda(m, \varepsilon)$ can be calculated by:

$$\lambda = \frac{v_p}{v_c} \left[\lambda_H^{\frac{m}{2}+2} \left(1 - \left(\frac{\lambda_w}{\lambda_H} \right)^2 \right)^{\frac{1}{2}} + (\pi \lambda_w \lambda_H)^{\frac{1}{2}} \frac{m \Gamma\left(\frac{m}{2} + \frac{1}{2}\right)}{\Gamma\left(\frac{m}{2} + 1\right)} \right] + \frac{v_w}{v_c} \lambda_w^{m/2}$$

where

$$v_p = \lambda_H v_H \left[1 + \frac{\lambda_w}{\lambda_H} \left(\frac{v_w}{v_H} \varepsilon \right)^2 \right]^{1/2}$$

$$v_c = \left(\lambda_H v_H^2 + \lambda_w v_w^2 \right)^{1/2}$$

$$\lambda_H = \sigma_{springing}^2 / \sigma_i^2$$

$$\lambda_w = \sigma_{wave}^2 / \sigma_i^2$$

$$v_H = f_{springing}$$

$$v_w = f_{wave}$$

$$\varepsilon = \sqrt{1 - \frac{\sigma_{wave-2}^4}{\sigma_{wave-0}^2 \sigma_{wave-4}^2}}$$

3 Time-Domain Approach for Fatigue Damage (1 June 2017)

This approach requires time-domain seakeeping analysis to calculate the time series of bending moment or stress considering the hull girder vibration due to springing. The stress ranges and number of cycles may be calculated from rainflow counting method, which is a recommended practice for the fatigue assessment of the hull structures subjected to the combined wave, and springing loads.

3.1 General

For the calculation of fatigue damage, the Palmgren-Miner's rule of damage accumulation may be used. For the one-slope S-N curve, the cumulative fatigue damage may be expressed by the following equation:

$$D = \sum_{i=1}^J \frac{n_i}{N_i} = \sum_{i=1}^J \frac{n_i}{K_2} S_i^m$$

where

$$n_i = \text{number of cycles of a stress range } S_i$$

$$N_i = \text{number of cycles to failure at the stress range } S_i$$

$$J = \text{number of stress range intervals}$$

$$S_i = \text{stress range}$$

- m = slope of the first segment of the S-N curve
- K_2 = constant relating to the first segment of the S-N curve

For the two-slope S-N curve, the cumulative fatigue damage may be expressed by the following equation:

$$D = \sum_{i=1}^J \frac{n_i}{N_i} = \sum_{i=1}^{J_q} \frac{n_i}{K_2} S_i^m + \sum_{i=J_q+1}^J \frac{n_i}{K_3} S_i^{m+2}$$

where

- n_i = number of cycles of a stress range S_i
- N_i = number of cycles to failure at the stress range S_i
- J = number of stress range intervals
- J_q = number of stress range intervals for $N_i < N_q$
- N_q = number of cycles ($=10^7$) at which the S-N curve has a change of slope from changes m to $m + 2$
- S_i = stress range
- m = slope of the first segment of the S-N curve
- K_3 = constant relating to the second segment of the S-N curve

The number of cycles for each stress range are to be calculated from the time series of the stress at each structural location for each sea state of the wave data.

3.2 Short-Term Fatigue Damage

A short-term fatigue damage may be calculated from the short-term probability of the stress ranges at particular locations of the vessel in a sea state. For a one-slope S-N curve, the short-term fatigue damage can be expressed:

$$D = \frac{N_T}{K_2} \sum_{i=1}^J p_i S_i^m$$

where

- p_i = short-term probability of stress range S_i
- N_T = total number of stress cycles

3.3 Long-Term Fatigue Damage

The long-term fatigue assessment may be carried out by combining all the short-term fatigue damages from each sea state considering the associated probability of occurrence of the sea state in the wave scatter table, which can be expressed as follows:

$$D_{LT} = \sum_{k=1}^M D_k p_k < 1$$

where

- D_k = short-term fatigue damage of the k -th sea state
- p_k = probability of occurrence of the k -th sea state
- M = total number of sea states

The time-domain approach to calculate the long-term fatigue damage considering all sea states and all wave headings may require time-consuming computations. As a simplified approach to reduce computational burden in the time-domain fatigue assessment, a head sea condition only may be considered to estimate the long-term fatigue damage factor. When a head sea condition only is considered, a heading factor of 0.5 may be used to estimate the long-term fatigue damage.

4 Fatigue Damage Assessment (1 June 2017)

4.1 Springing Contribution to Fatigue Damage

The springing fatigue damage contribution can be evaluated by the ratio of springing-induced damage to the damage by wave frequency load as:

$$\alpha_s = 1 + \frac{D_{total} - D_{wave}}{D_{wave}}$$

where

$$\begin{aligned}\alpha_s &= \text{fatigue damage factor including springing} \\ D_{total} &= \text{total fatigue damage including springing} \\ D_{wave} &= \text{fatigue damage due to wave frequency load}\end{aligned}$$

The fatigue damage factors from loading conditions selected according to Subsection 2/2 can be combined through weighted average based on the probability of operation duration of each loading condition.

4.2 Fatigue Damage Assessment

As mentioned above, the objective of the fatigue assessment is to obtain the relative contribution to the fatigue damage attributable to springing. The result can be used in the total fatigue damage calculation where it is applicable, such as in the *ABS Guide for Application of Higher-Strength Hull Structural Thick Steel Plates in Container Carriers*. In the aforementioned Guide, the cumulative fatigue damage, D_p is to be taken as:

$$D_f = \frac{1}{6} \alpha_s \alpha_w (D_{f_{12}} + D_{f_{34}}) + \frac{1}{3} D_{f_{56}} + \frac{1}{3} D_{f_{78}} \leq 0.8$$

where

$$\begin{aligned}\alpha_w &= \text{fatigue damage factor including whipping} \\ \alpha_s &= \text{fatigue damage factor including springing}\end{aligned}$$

$D_{f_{12}}$, $D_{f_{34}}$, $D_{f_{56}}$, and $D_{f_{78}}$ are the fatigue damage accumulated due to load case pairs 1 & 2, 3 & 4, 5 & 6 and 7 & 8, respectively. The detailed procedures for the calculation for $D_{f_{12}}$, $D_{f_{34}}$, $D_{f_{56}}$, and $D_{f_{78}}$ are given in Appendix 1.



APPENDIX 1 Fatigue Strength Assessment

1 General

1.1 **Note (1 June 2017)**

Rules) provide a design oriented approach to fatigue strength assessment which may be used, for certain structural details, in lieu of more elaborate methods such as spectral fatigue analysis. This Appendix offers specific guidance on a full ship finite element based fatigue strength assessment of certain structural details in the upper flange of hull structure. For other structural details, Appendix 5C-5-A1 “Fatigue Strength Assessment of Container Carriers” and 5C-3-A1 “Fatigue Strength Assessment of Bulk Carriers” of the *Steel Vessel Rules* provide the detailed procedures. The term “assessment” is used here to distinguish this approach from the more elaborate analysis.

Under the design torsional moment curves defined in 5C-5-3/5.1.5 and 5C-3-3/5.3.3 of the *Steel Vessel Rules*, the warping stress distributions can be accurately determined from a full ship finite element model for container and ore carrier configurations, for example:

- Engine room and deckhouse co-located amidships
- Engine room and deckhouse that are separately located
- Fuel oil tanks located within cargo tanks

The full ship finite element based fatigue strength assessment is considered an essential step in evaluating hull structural thick steel plates in large container carriers.

The criteria in this Appendix are developed from various sources, including the Palmgren-Miner linear damage model, S-N curve methodologies, long-term environment data of the North-Atlantic Ocean, etc., and assume workmanship of commercial marine quality acceptable to the Surveyor.

1.2 **Applicability (1 June 2017)**

The criteria in this Appendix are specifically written for container and ore carriers to which Part 5C, Chapter 5 and Part 5C, Chapter 3 of the *Steel Vessel Rules* are applicable.

1.3 **Loadings**

The criteria have been written for ordinary wave-induced motions and loads. Other cyclic loadings, which may result in significant levels of stress ranges over the expected lifetime of the vessel, are also to be considered by the designer.

Where it is known that a vessel will be engaged in long-term service on a route with a more severe environment, the fatigue strength assessment criteria in these Guidance Notes are to be modified accordingly.

1.4 **Effects of Corrosion**

To account for the mean wastage throughout the service life, the total stress range calculated from a full ship finite element model using the gross scantlings is modified by a factor c_f . See A1/5.2.1.

1.5 **Format of the Criteria**

The criteria in this Appendix are presented as a comparison of fatigue strength of the structure (capacity) and fatigue inducing loads (demands) as represented by the calculated cumulative fatigue damage over the design service life of 20 years in the North Atlantic Ocean. In other words, the calculated cumulative fatigue damage is to be not less than 0.8.

2 Connections to be Considered for the Fatigue Strength Assessment

2.1 General (1 June 2017)

The criteria in this Appendix have been developed to allow consideration of a broad variation of structural details and arrangements in the upper flange of hull structure so that most of the important structural details anywhere in the vessel can be subjected to an explicit (numerical) fatigue assessment using these criteria. However, where justified by comparison with details proven satisfactory under equal or more severe conditions, an explicit assessment can be exempted.

2.2 Guidance on Locations for Container Carriers (1 June 2017)

As a general guidance for assessing fatigue strength for a container carrier, the following connections and locations are to be considered:

2.2.1 Hatch Corners

The following locations of hatch corners:

2.2.1(a) Typical hatch corners within $0.4L$ amidships

2.2.1(b) Hatch corners at the forward cargo hold

2.2.1(c) Hatch corners immediately forward and aft of the engine room

2.2.1(d) Hatch corners immediately forward and aft of the accommodation block, if it is not co-located with the engine room

2.2.1(e) Hatch corners subject to significant warping constraint from the adjacent structures

2.2.2 Connection of Longitudinal Hatch Girders and Cross Deck Box Beams to Other Supporting Structures

Representative locations of each hatch girder and cross deck box beam connection.

2.2.3 Representative Cut-outs

Representative cut-outs in the longitudinal bulkheads, longitudinal deck girder, hatch side coamings, and cross deck box beams.

2.2.4 Other Regions and Locations

Other regions and locations highly stressed by fluctuating loads, as identified from the full ship finite element torsional analysis.

2.3 Guidance on Locations for Ore Carriers (1 June 2017)

As a general guidance for assessing fatigue strength for an ore carrier, the following connections and locations are to be considered:

2.3.1 Hatch Corners

The following locations of hatch corners:

2.3.1(a) Typical hatch corners within $0.4L$ amidships

2.3.1(b) Hatch corners at the forward cargo hold

2.3.1(c) Hatch corners immediately forward and aft of the engine room

2.3.1(d) Hatch corners immediately forward and aft of the accommodation block, if it is not co-located with the engine room

2.3.1(e) Hatch corners subject to significant warping constraint from the adjacent structures

2.3.2 Connections of Hold Frame

All typical end connections of hold frames to the upper and lower wing tanks in the ballast, heavy cargo and general cargo holds.

2.3.3 Connection of Longitudinal Stiffeners to Transverse Web/Floor and Transverse Bulkhead

2.3.3(a) Two (2) to three (3) selected side longitudinals in the upper and lower wing tanks for the midship region and also in the region between $0.15L$ and $0.25L$ from the FP

2.3.3(b) One (1) to two (2) selected longitudinals from each of the following groups:

- Deck longitudinals, bottom longitudinals, inner bottom longitudinals and longitudinals on the slope/longitudinal bulkheads.
- One longitudinal on the inner skin longitudinal bulkhead within $0.10D$ from the deck is to be included.

2.3.4 Shell, Bottom or Bulkhead Plating at Connections to the Sloping Longitudinal Bulkhead Plating, Transverse Webs or Floors

2.3.4(a) One (1) to two (2) selected locations of side shell plating at connections of the sloping bulkhead plating and hold frames, and near the summer *LWL* amidships, and also between $0.15L$ and $0.25L$ from the FP

2.3.4(b) One (1) to two (2) selected locations in way of bottom, inner bottom and lower strakes of the sloping longitudinal bulkhead of the lower wing tanks amidships, respectively.

2.3.5 Other Regions and Locations

Other regions and locations highly stressed by fluctuating loads, as identified from the full ship finite element torsional analysis.

For the structural details identified above, the stress concentration factor (SCF) may be calculated by the approximate equations given in Subsection A1/5. Alternatively, the stress concentration factor (SCF) may be determined from fine mesh F.E.M. analyses (see Subsection A1/6).

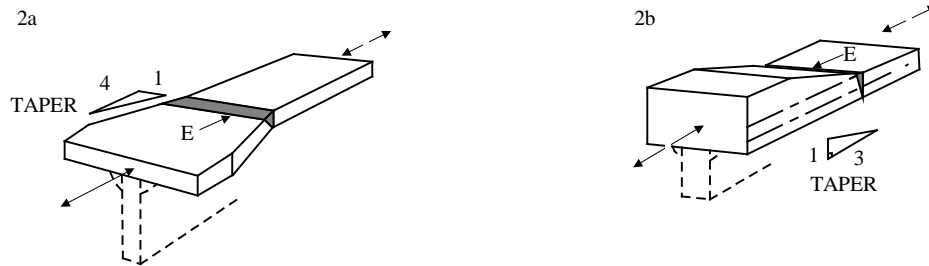
2.4 Fatigue Classification

2.4.1 Welded Connections with One Load Carrying Member

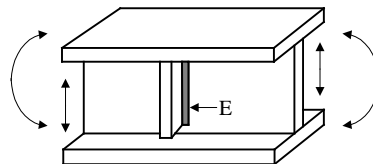
Fatigue classification for structural details is shown in Appendix 1, Table 1.

TABLE 1
Fatigue Classification for Structural Details

<i>Class Designation</i>	<i>Description</i>
B	Parent materials, plates or shapes as-rolled or drawn, with no flame-cut edges. In case with any flame-cut edges, the flame-cut edges are subsequently ground or machined to remove all visible sign of the drag lines
C	<ol style="list-style-type: none"> 1) Parent material with automatic flame-cut edges 2) Full penetration seam welds or longitudinal fillet welds made by an automatic submerged or open arc process, and with no stop-start positions within the length.
D	<ol style="list-style-type: none"> 1) Full penetration butt welds made either manually or by an automatic process other than submerged arc, from both sides, in downhand position. 2) Weld in C-2) with stop-start positions within the length
E	<ol style="list-style-type: none"> 1) Full penetration butt welds made by other processes than those specified under D-1) 2) Full penetration butt welds made from both sides between plates of unequal widths or thicknesses



- 3) Welds of brackets and stiffeners to web plate of girders



- F**
- 1) Full penetration butt weld made on a permanent backing strip
 - 2) Rounded fillet welds as shown below

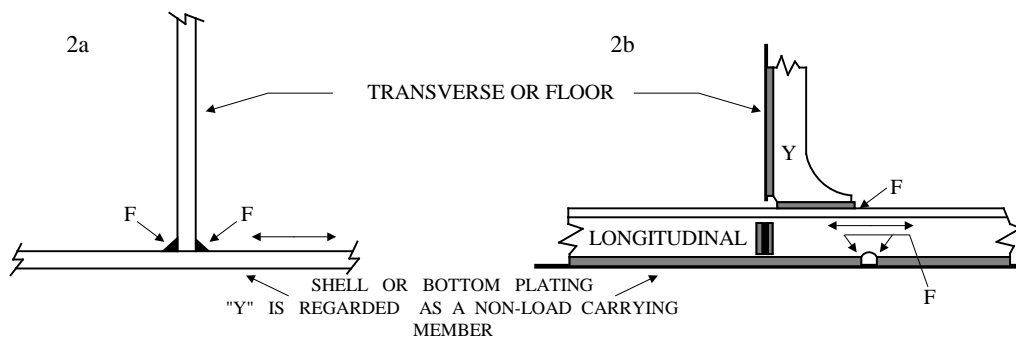
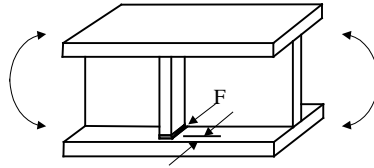


TABLE 1 (continued)
Fatigue Classification for Structural Details

Class Designation

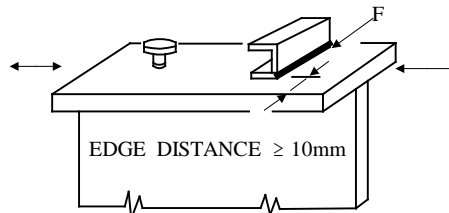
Description

- 3) Welds of brackets and stiffeners to flanges



EDGE DISTANCE $\geq 10\text{mm}$

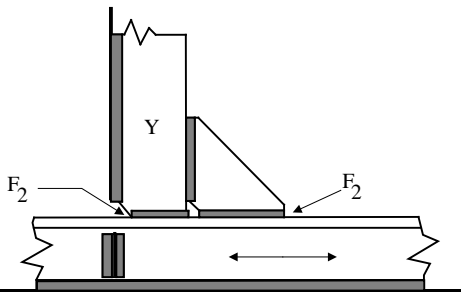
- 4) Attachments on plate or face plate



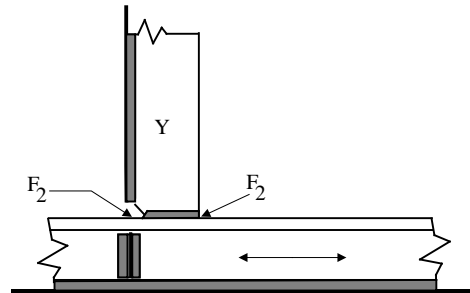
(Class G for edge distance $< 10\text{ mm}$)

- F₂** 1) Fillet welds as shown below with rounded welds and no undercutting

1a



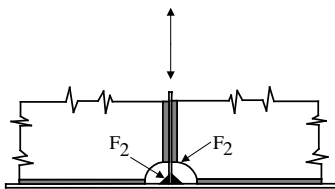
1b



"Y" is a non-load carrying member

- 2) Fillet welds with any undercutting at the corners dressed out by local grinding

2a)



2b)

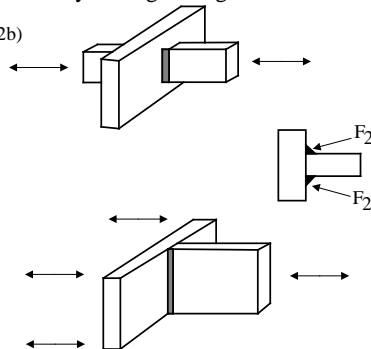
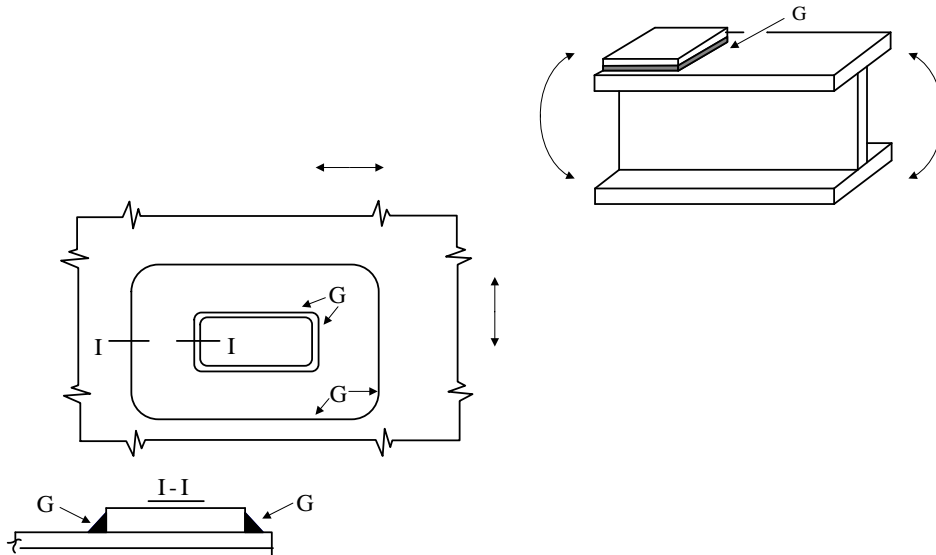
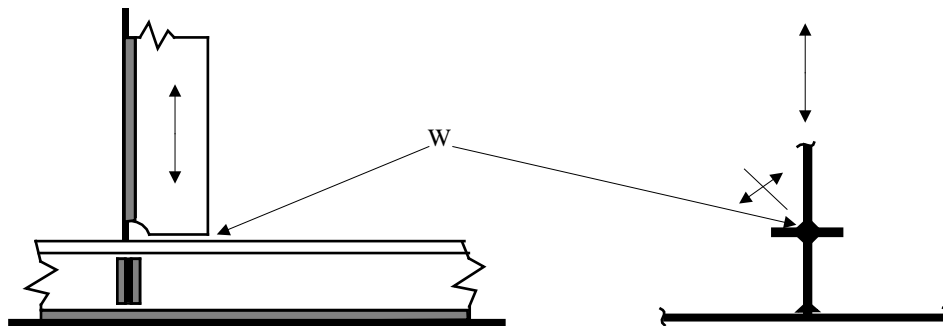


TABLE 1 (continued)
Fatigue Classification for Structural Details

<i>Class Designation</i>	<i>Description</i>
G	1) Fillet welds in F ₂ - 1) without rounded toe welds or with limited minor undercutting at corners or bracket toes 2) Fillet welds in F ₂ - 2) with minor undercutting 3) Doubler on face plate or flange, small deck openings 4) Overlapped joints as shown below



W	1) Fillet welds in G - 3) with any undercutting at the toes 2) Fillet welds – weld throat
----------	----------------------------------------------------------------------------------------------

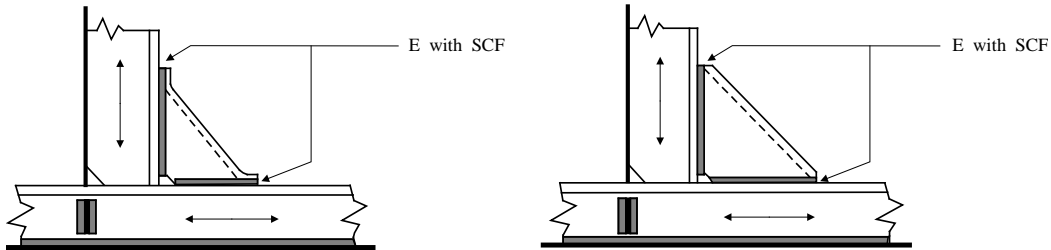


2.4.2 Welded Joint with Two or More Load Carrying Members

For brackets connecting two or more load carrying members, an appropriate stress concentration factor (SCF) determined from fine mesh finite element analysis is to be used. In this connection, the fatigue class at bracket toes may be upgraded to class E. Sample connections are illustrated below with/without SCF.

TABLE 2
Welded Joint with Two or More Load Carrying Members
for Container Carriers (1 June 2017)

a Connections of Longitudinal and Stiffener



b Connections of Longitudinal Deck Girders and Cross Deck Box

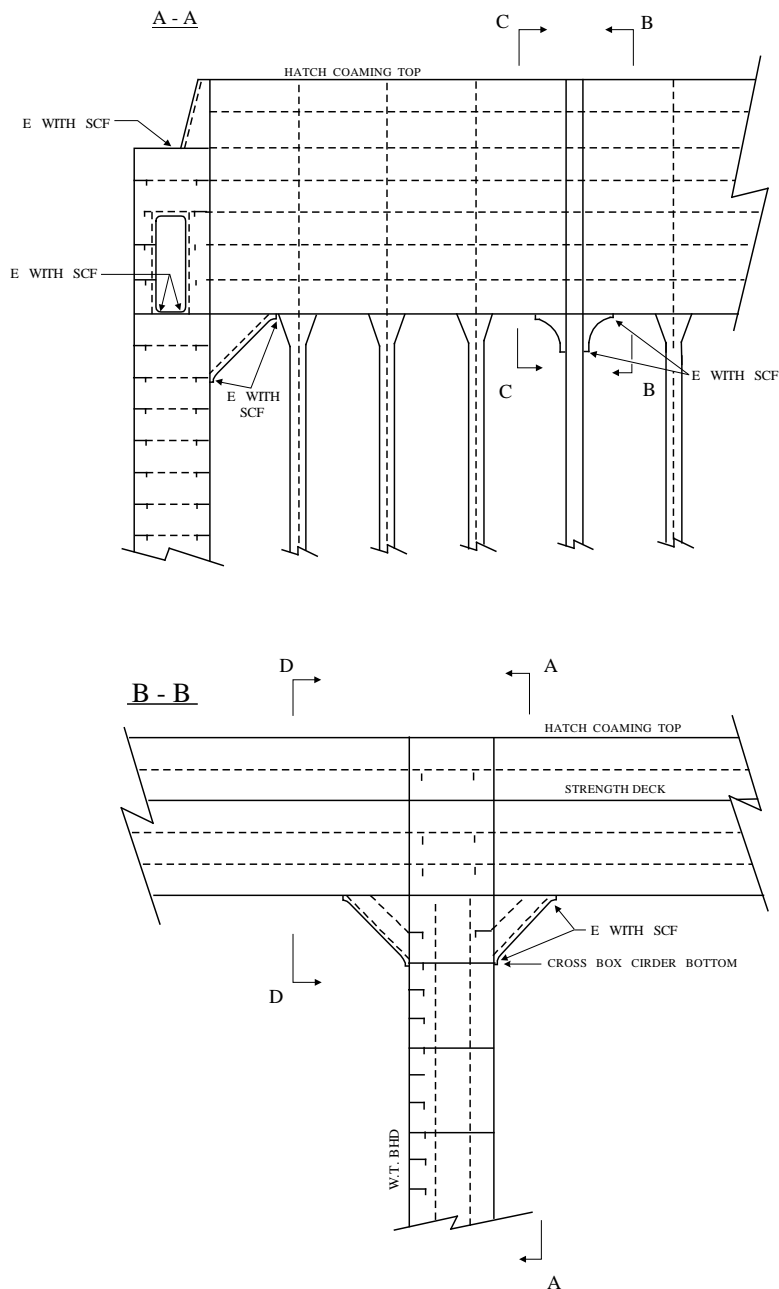
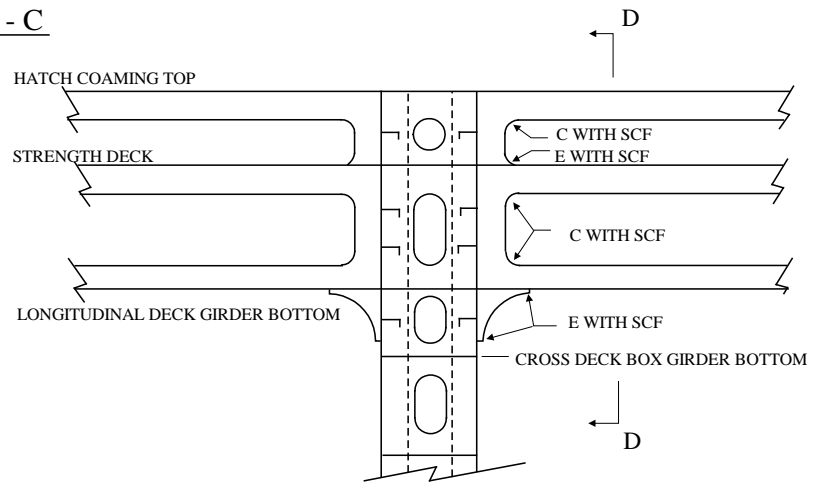


TABLE 2 (continued)
Welded Joint with Two or More Load Carrying Members
for Container Carriers (1 June 2017)

C - C



D - D

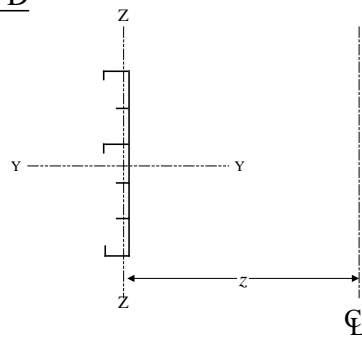
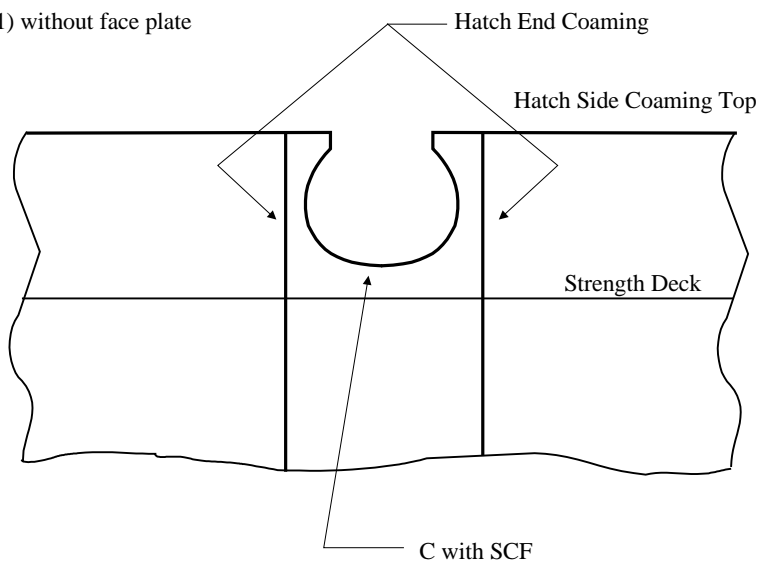


TABLE 2 (continued)
Welded Joint with Two or More Load Carrying Members
for Container Carriers (1 June 2017)

c Discontinuous Hatch Side Coaming

1) without face plate



2) with face plate

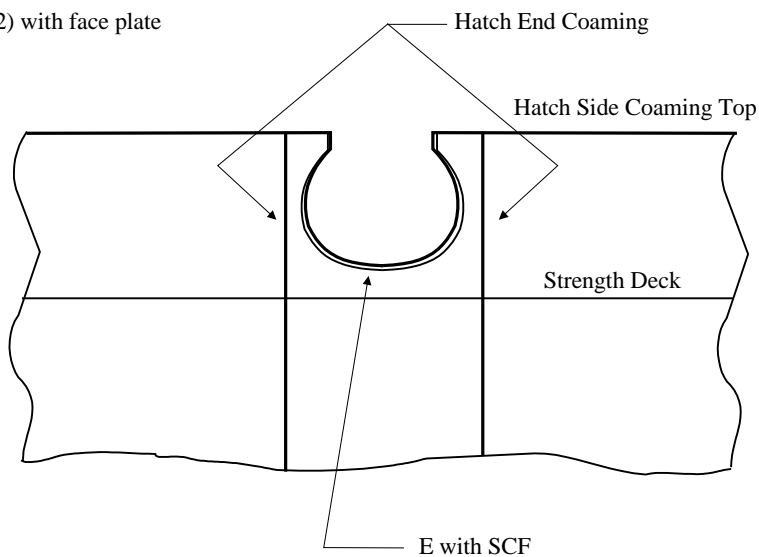
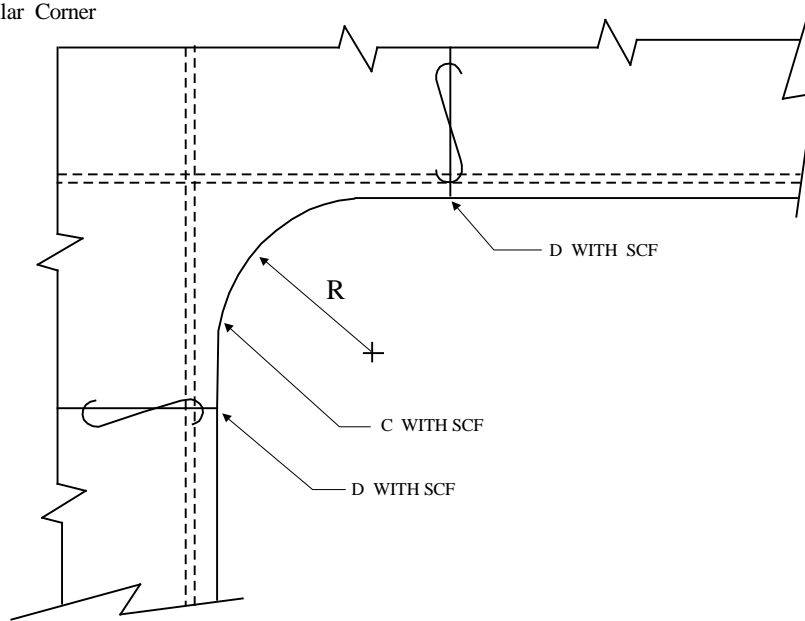


TABLE 2 (continued)
Welded Joint with Two or More Load Carrying Members
for Container Carriers (1 June 2017)

d Hatch Corners

Circular Corner



Double Curvature

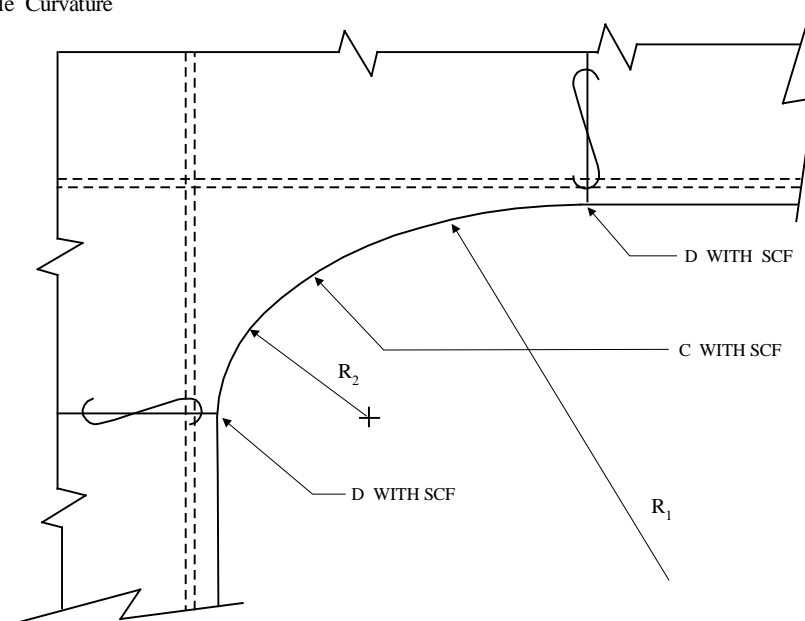


TABLE 2 (continued)
Welded Joint with Two or More Load Carrying Members
for Container Carriers (1 June 2017)

Cut-out Radius

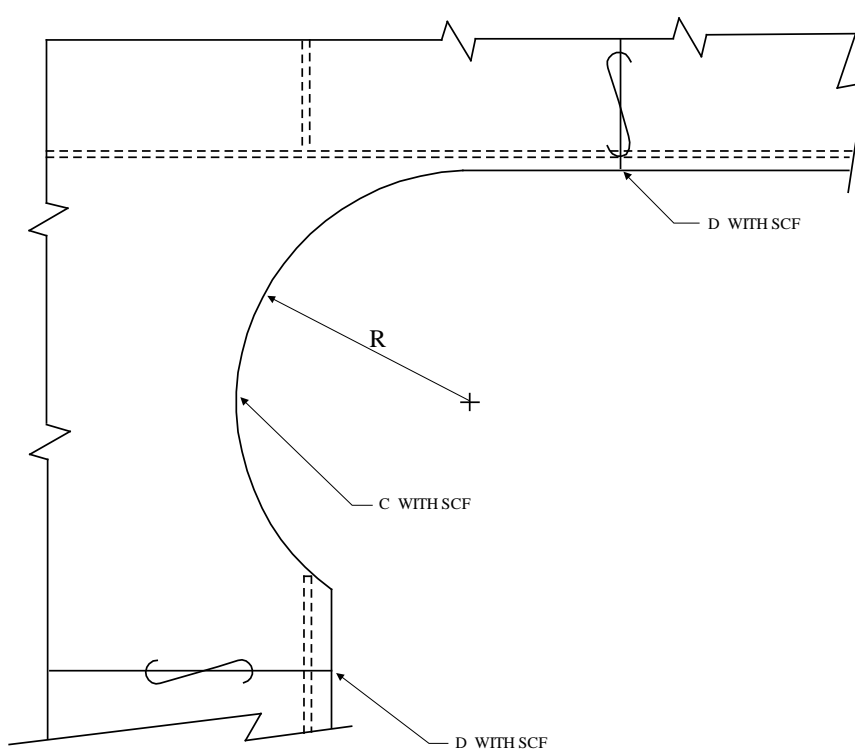
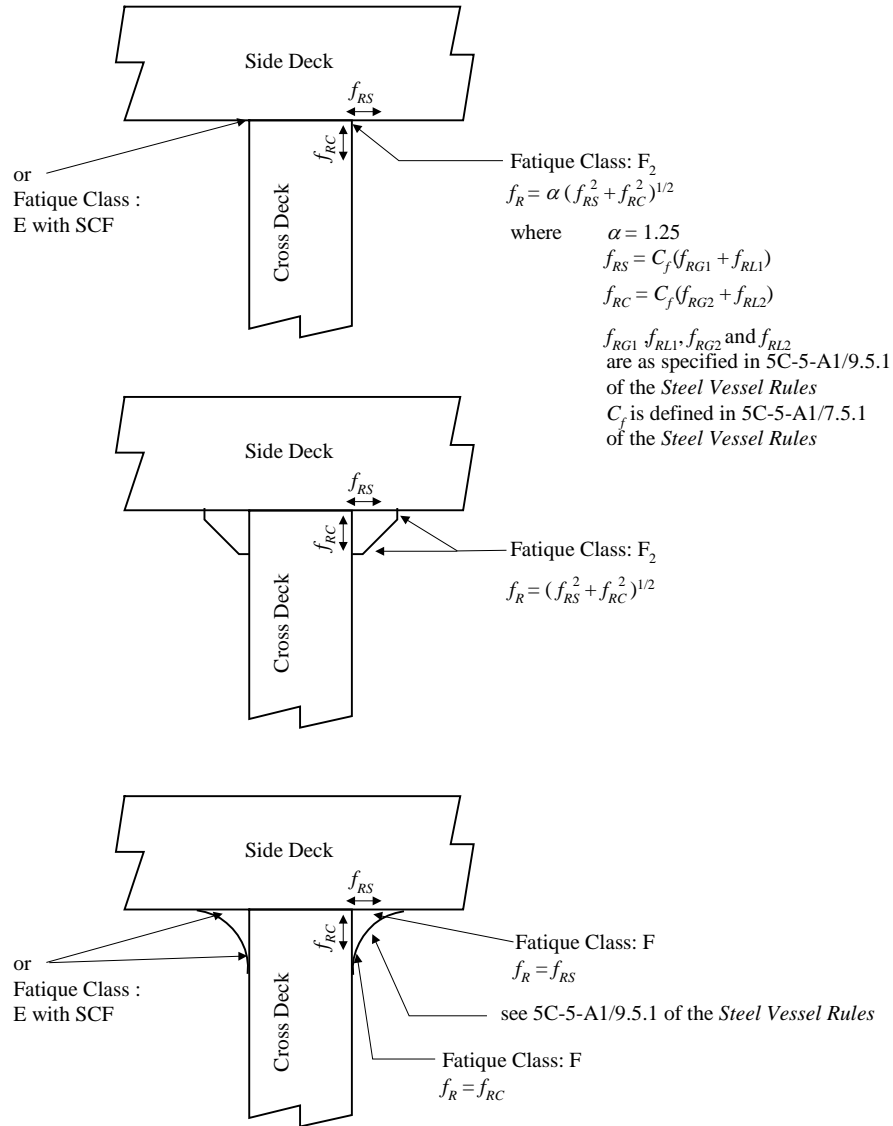


TABLE 2 (continued)
Welded Joint with Two or More Load Carrying Members
for Container Carriers (1 June 2017)

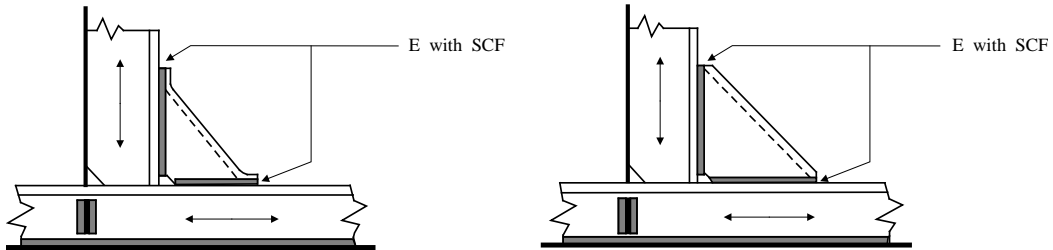
End Connections at Lower Deck



Note: Thickness of brackets is to be not less than that of cross deck plating in the same location (level).
 For fitting of cell guide, no cut nor welding to the brackets is allowed.

TABLE 3
Welded Joint with Two or More Load Carrying Members
for Ore Carriers (1 June 2017)

a Connections of Longitudinal and Stiffener



b Connections between Corrugated Transverse Bulkhead and Deck

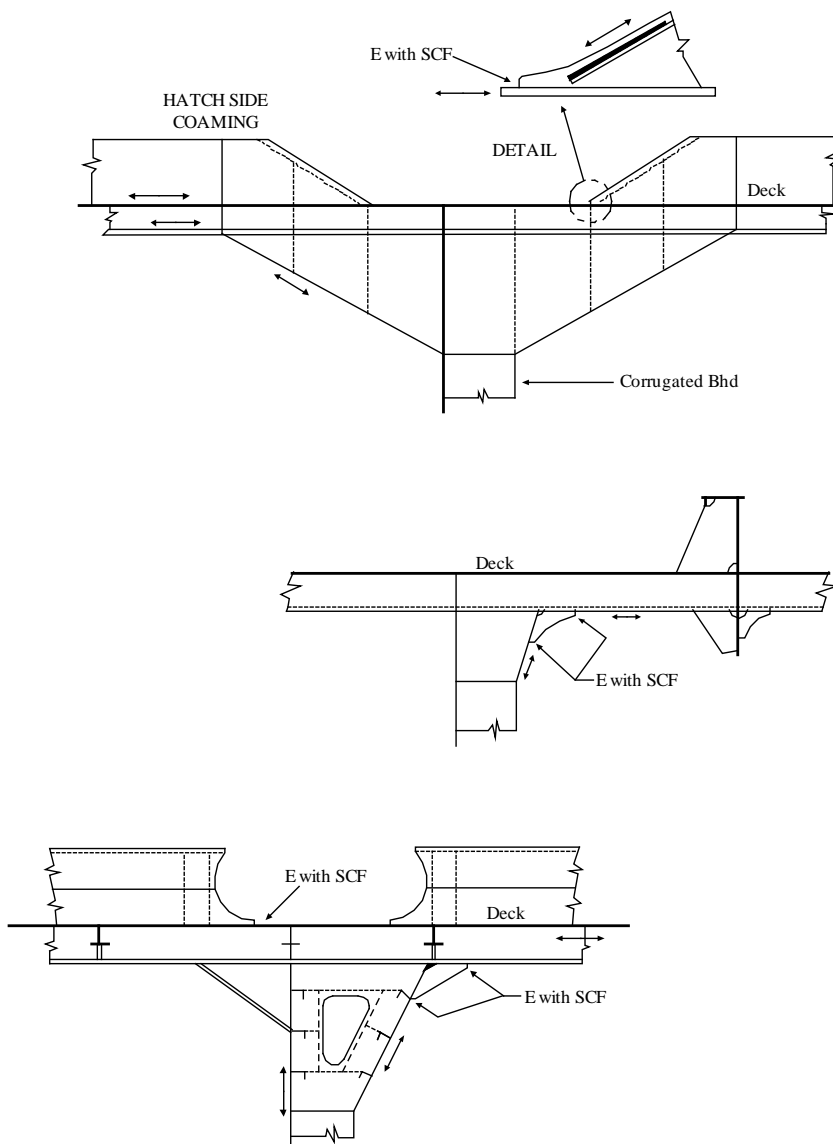
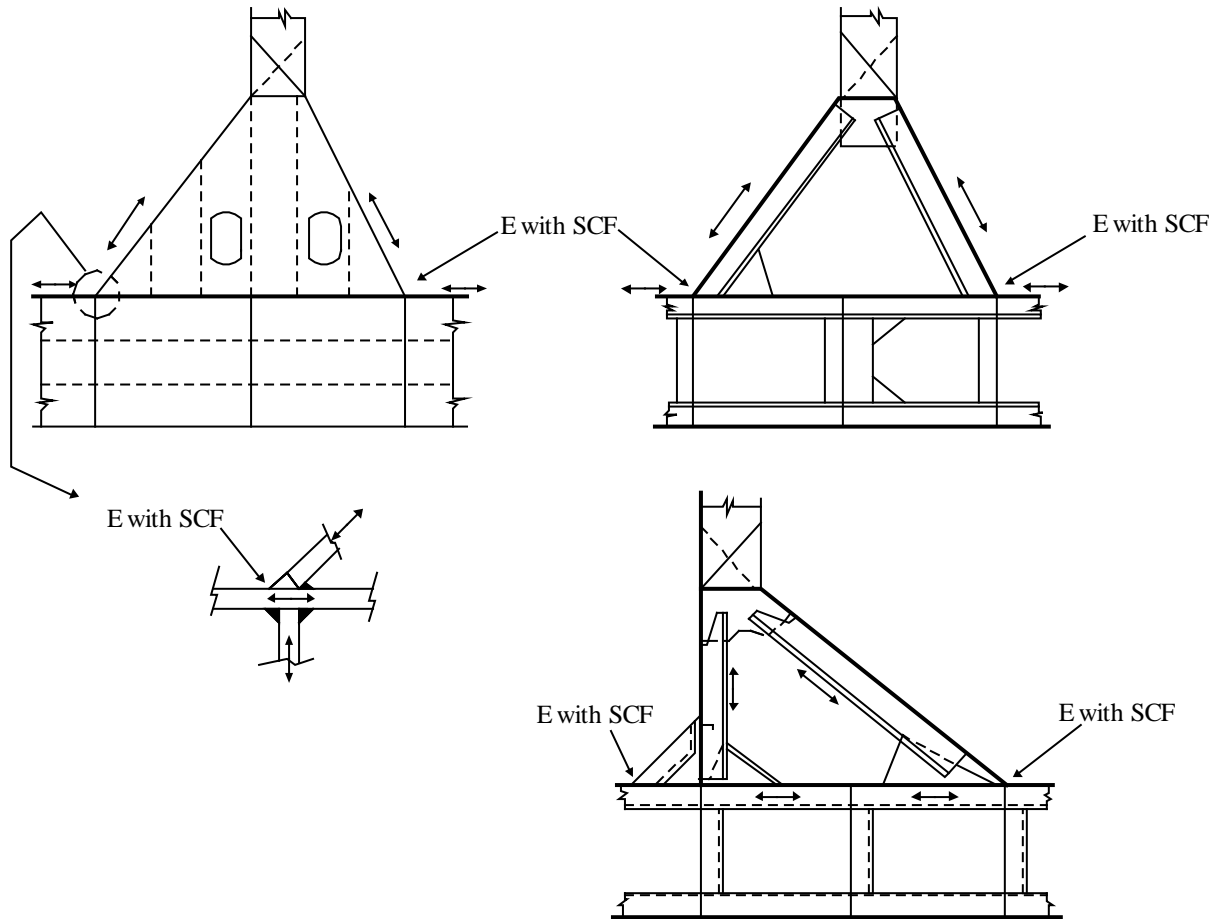


TABLE 3 (continued)
Welded Joint with Two or More Load Carrying Members
for Ore Carriers (1 June 2017)

c Connections between Corrugated Transverse Bulkhead and Inner Bottom with Respect to Lateral Load on the Bulkhead



d Connections between Inner Bottom and Hopper Tank Slope

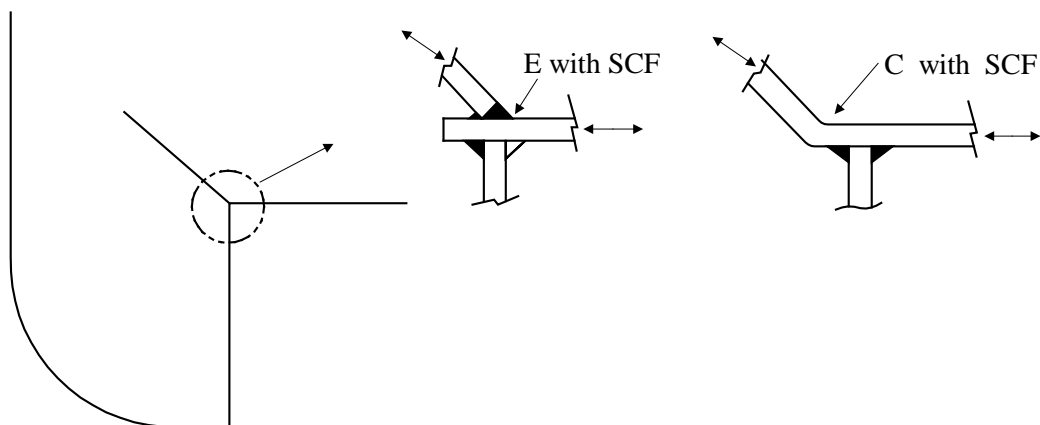
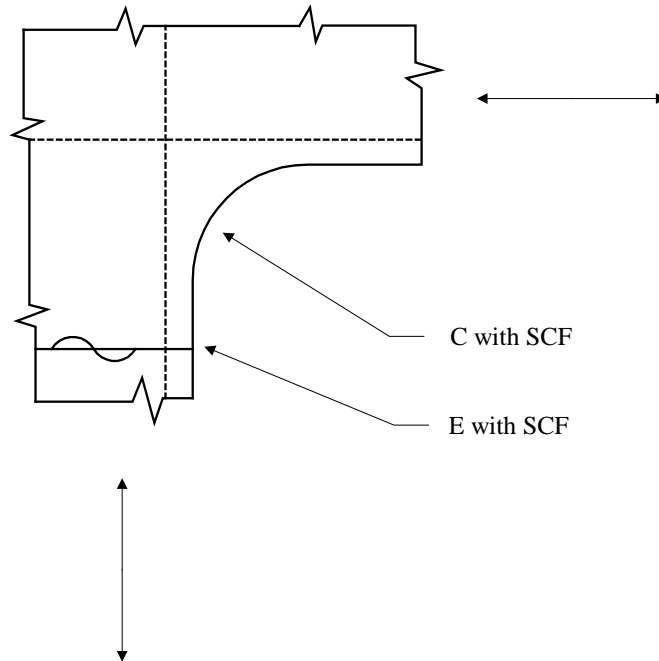


TABLE 3 (continued)
Welded Joint with Two or More Load Carrying Members
for Ore Carriers (1 June 2017)

e Hatch Corner



3 Fatigue Damage Calculation

3.1 Assumptions

The fatigue damage of a structural detail under the loads specified here is to be evaluated using the criteria contained in this Subsection. The key assumptions employed are listed below for guidance.

- A linear cumulative damage model (i.e., Palmgren-Miner’s Rule) has been used in connection with the S-N data in Appendix 1, Figure 1 (extracted from Ref. 1*).
- * Ref. 1: “Offshore Installations: Guidance on Design, Construction and Certification”, Department of Energy, U.K., Fourth Edition - 1990, London: HMSO
- Cyclic stresses due to the loads in Subsection A1/5 have been used, and the effects of mean stress have been ignored.
- The target design life of the vessel is taken to be 20 years.
- The long-term stress ranges on a detail can be characterized by using a modified Weibull probability distribution parameter (γ).
- Structural details are classified and described in Appendix 1, Table 1, “Fatigue Classification for Structural Details”.

The structural detail classification in Appendix 1, Table 1 is based on joint geometry and direction of the dominant load. Where the loading or geometry is too complex for a simple classification, a finite element analysis of the details is to be carried out to determine the stress concentration factors. Subsection A1/6 contains guidance on finite element analysis modeling to determine stress concentration factors for weld toe locations that are typically found at longitudinal stiffener end connections.

3.2 Criteria

The fatigue damage, D_f , obtained using the criteria in A1/3.4, is to be not greater than 0.8.

3.3 Long Term Stress Distribution Parameter, γ

The long-term stress distribution parameter, γ , can be determined as shown below:

$$\gamma = \alpha \left(1.1 - 0.35 \frac{L - 100}{300} \right)$$

where

α	=	1.0	for deck structures, including side shell and longitudinal bulkhead structures within $0.1D$ from the deck
	=	1.05	for bottom structures, including inner bottom and side shell, and longitudinal bulkhead structures within $0.1D$ from the bottom
	=	1.1	for side shell and longitudinal bulkhead structures within the region of $0.25D$ upward and $0.3D$ downward from the mid-depth
	=	1.1	for transverse bulkhead structures

α may be linearly interpolated for side shell and longitudinal bulkhead structures between $0.1D$ and $0.25D$ from the deck, and between $0.1D$ and $0.2D$ from the bottom.

L = vessel's length, as defined in 3-1-1/3.1 of the *Steel Vessel Rules*.

D = vessel's depth, as defined in 3-1-1/7 of the *Steel Vessel Rules*.

3.4 Fatigue Damage (1 June 2017)

The cumulative fatigue damage, D_f , is to be taken as:

$$D_f = \frac{1}{6} \alpha_s \alpha_w (D_{f_{12}} + D_{f_{34}}) + \frac{1}{3} D_{f_{56}} + \frac{1}{3} D_{f_{78}} \leq 0.8$$

where

α_s = fatigue damage factor due to hull girder springing. α_s is the ratio of the fatigue damage of a flexible hull girder and that of a rigid body hull girder due to wave-induced vertical bending moment in head or rear seas. If the effect of hull girder springing is ignored, α_s is equal to 1.0. For a flexible hull girder structure, α_s is greater than 1.0. α_s is to be determined based on well documented experimental data or analytical studies. When these direct calculations are not available, α_s may be conservatively taken as 1.3.

α_w = fatigue damage factor due to hull girder whipping. α_w is the ratio of the fatigue damage of a flexible hull girder and that of a rigid body hull girder due to wave-induced vertical bending moment in head or rear seas. If the effect of hull girder whipping is ignored, α_w is equal to 1.0. For a flexible hull girder structure, α_w is greater than 1.0. α_w is to be determined based on well documented experimental data or analytical studies. When these direct calculations are not available, α_w may be conservatively taken as 1.3.

$D_{f_{12}}$, $D_{f_{34}}$, $D_{f_{56}}$ and $D_{f_{78}}$ are the fatigue damage accumulated due to load case pairs 1 & 2, 3 & 4, 5 & 6 and 7 & 8, respectively (see Subsection A1/4 for load case pairs).

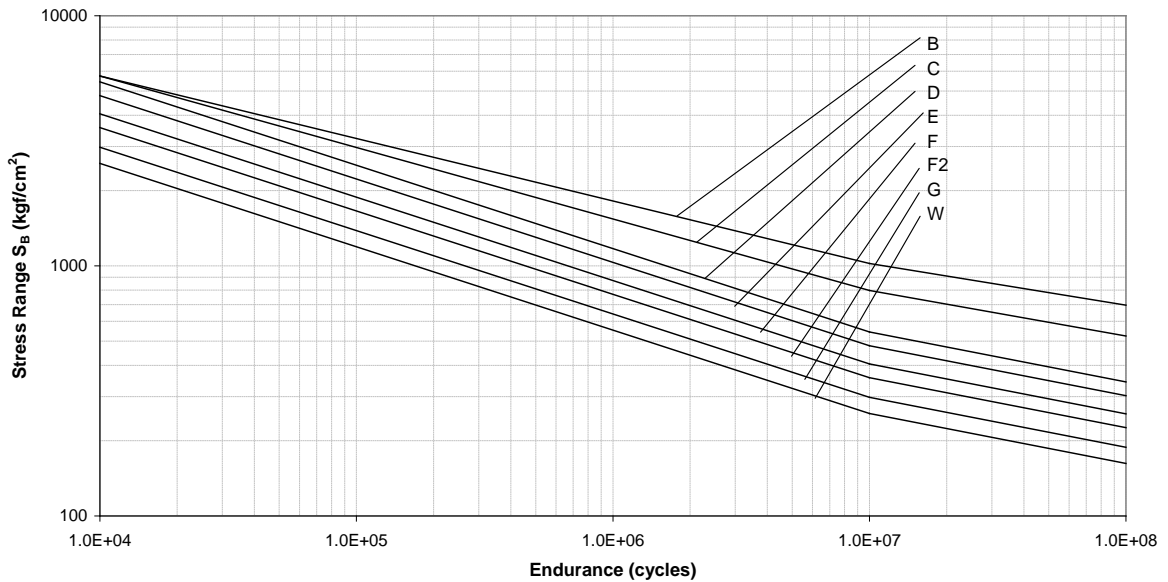
Assuming the long term distribution of stress ranges follow the Weibull distribution, the fatigue damage accumulated due to load pair jk is:

$$D_{f_{jk}} = \frac{N_T}{K_2} \frac{(k_t k_h f_{R_{jk}})^m}{(\ln N_R)^{m/\gamma}} \mu_{jk} \Gamma \left(1 + \frac{m}{\gamma} \right)$$

where

- N_T = number of cycles in the design life
 = $\frac{f_0 D_L}{4 \log L}$
- f_0 = 0.85, factor for net time at sea
- D_L = design life in seconds, 6.31×10^8 for a design life of 20 years
- L = vessel length defined in 3-1-1/3.1 of the *Steel Vessel Rules*
- m, K_2 = S-N curve parameters, as defined in Appendix 1, Figure 1 of these Guidance Notes
- f_{R-jk} = stress range of load case pair jk at the representative probability level of 10^{-4} , in kgf/cm^2 (lbf/in^2)
- k_t = thickness correction factor
 = $\left(\frac{t}{22}\right)^n$ for $t \geq 22$ mm, where t is the plate thickness
 = 1 for $t < 22$ mm
- n = 0.20 for a transverse butt weld with its upper and lower edges as built or ground to 1C
 = 0.10 for a transverse butt weld with its upper and lower edges ground with a radius of 3 ~ 5 mm. The extent of the grinding is to be 100 mm forward and aft of the butt weld as shown in Appendix 1, Table 1.
 = 0.10 for hatch corner insert plate away from the welds. The upper and lower edges are ground with a radius of 3 ~ 5 mm
- k_h = correction factor for higher-strength steel, applicable to parent material only
 = 1.000 for mild steel or welded connections
 = 0.926 for H32 steel
 = 0.885 for H36 steel
 = 0.870 for H40 steel
 = 0.850 for H47 steel
- N_R = 10000, number of cycles corresponding to the probability level of 10^{-4}
- γ = long-term stress distribution parameter as defined in A1/3.3
- Γ = Complete Gamma function
- μ_{jk} =
$$1 - \frac{\left\{ \Gamma_0 \left(1 + \frac{m}{\gamma}, v_{jk} \right) - v_{jk}^{-\Delta m / \gamma} \Gamma_0 \left(1 + \frac{m + \Delta m}{\gamma}, v_{jk} \right) \right\}}{\Gamma \left(1 + \frac{m}{\gamma} \right)}$$
- v_{jk} =
$$\left(\frac{f_q}{f_{R-jk}} \right)^\gamma \ln N_R$$
- f_q = stress range at the intersection of the two segments of the S-N curve in kgf/cm^2 -(lbf/in^2)
- Δm = 2, slope change of the upper-lower segment of the S-N curve
- $\Gamma_0(\)$ = incomplete Gamma function, Legendre form

FIGURE 1
Basic Design S-N Curves (1 June 2017)



Notes for Figure 1:

Basic design S-N curves

The basic design curves consist of linear relationships between $\log(S_B)$ and $\log(N)$. They are based upon a statistical analysis of appropriate experimental data and may be taken to represent two standard deviations below the mean line. Thus the basic S-N curves for $N \leq 10^7$ are of the form:

$$\log(N) = \log(K_2) - m \log(S_B)$$

where

$$\log(K_2) = \log(K_1) - 2\sigma$$

N = predicted number of cycles to failure under stress range S_B

K_1 = a constant relating to the mean S-N curve

σ = standard deviation of $\log N$

m = inverse slope of the S-N curve

K_2 = a constant relating to the first segment of the S-N curve

The S-N curves for $N > 10^7$ are of the form:

$$\log(N) = \log(K_3) - (m + 2) \log(S_B)$$

where

$$\log(K_3) = \log(K_2) - 2 \log(f_q)$$

K_3 = a constant relating to the second segment of the S-N curve

f_q = stress range at the intersection of the two segments of the S-N curve

The relevant values of these terms are shown in the table below and stress range is in kgf/cm^2 . The S-N curves have a change of inverse slope from m to $m + 2$ at $N = 10^7$ cycles.

FIGURE 1 (continued)
Basic Design S-N Curves (1 June 2017)

Class	K_1	σ	m	K_2	f_a (kgf/cm ²)	$m+2$	K_3
B	2.521×10^{19}	0.1821	4.0	1.090×10^{19}	1021.778	6.0	1.138×10^{25}
C	3.660×10^{17}	0.2041	3.5	1.430×10^{17}	797.122	5.5	9.085×10^{22}
D	4.225×10^{15}	0.2095	3.0	1.610×10^{15}	544.012	5.0	4.765×10^{20}
E	3.493×10^{15}	0.2509	3.0	1.100×10^{15}	479.142	5.0	2.525×10^{20}
F	1.825×10^{15}	0.2183	3.0	6.678×10^{14}	405.750	5.0	1.099×10^{20}
F₂	1.302×10^{15}	0.2279	3.0	4.558×10^{14}	357.263	5.0	5.818×10^{19}
G	6.051×10^{14}	0.1793	3.0	2.650×10^{14}	298.137	5.0	2.355×10^{19}
W	3.978×10^{14}	0.1846	3.0	1.700×10^{14}	257.128	5.0	1.124×10^{19}

4 Fatigue Inducing Loads and Load Combination Cases

4.1 General (1 June 2017)

This Subsection provides: 1) the criteria to define the individual load components considered to cause fatigue damage in the upper flange of a hull structure (see A1/4.2); 2) the load combination cases to be considered for the upper flange of the hull structure containing the structural detail being evaluated (see A1/4.3).

4.2 Wave-induced Loads

The fluctuating load components to be considered are those induced by the seaway. They are divided into the following three groups:

- Hull girder wave-induced vertical bending moment
- Hull girder wave-induced horizontal bending moment
- Hull girder wave-induced torsional moment

4.3 Combinations of Load Cases for Fatigue Assessment (1 June 2017)

A loading condition is considered in the calculation of stress range. For this loading condition, eight (8) load cases, as shown in Appendix 1, Tables 4 and 5, are defined to form four (4) pairs. The combinations of load cases are to be used to find the characteristic stress range corresponding to a probability of exceedance of 10^{-4} , as indicated below.

TABLE 4
Combined Load Cases for Fatigue Strength Formulation
for Container Carriers (1 June 2017)

	L.C. 1	L.C. 2	L.C. 3	L.C. 4	L.C. 5	L.C. 6	L.C. 7	L.C. 8
Wave Induced Vertical Bending Moment	Sag 100%	Hog 100%	Sag 70%	Hog 70%	Sag 30%	Hog 30%	Sag 40%	Hog 40%
Wave Induced Horizontal Bending Moment	0.0	0.0	0.0	0.0	Stbd Tens 30%	Port Tens 30%	Stbd Tens 50%	Port Tens 50%
Wave Induced Torsional Moment	0.0	0.0	0.0	0.0	(-) 55%	(+) 55%	(-) 100%	(+) 100%
Wave Heading Angle	Head & Follow	Head & Follow	Head & Follow	Head & Follow	Beam	Beam	Oblique	Oblique

Notes:

- 1 Wave induced vertical bending moment is defined in 5C-5-3/5.1.1 of the *Steel Vessel Rules*.
- 2 Wave induced horizontal bending moment is defined in 5C-5-3/5.1.3 of the *Steel Vessel Rules*.
- 3 Wave induced torsional moment and sign convention are defined in 5C-5-3/5.1.5 of the *Steel Vessel Rules*.

TABLE 5
Combined Load Cases for Fatigue Strength Formulation
for Ore Carriers (1 June 2017)

	<i>L.C. 1</i>	<i>L.C. 2</i>	<i>L.C. 3</i>	<i>L.C. 4</i>	<i>L.C. 5</i>	<i>L.C. 6</i>	<i>L.C. 7</i>	<i>L.C. 8</i>
Wave Induced Vertical Bending Moment	Sag 100%	Hog 100%	Sag 70%	Hog 70%	Sag 30%	Hog 30%	Sag 40%	Hog 40%
Wave Induced Horizontal Bending Moment	0.0	0.0	0.0	0.0	Stbd Tens 30%	Port Tens 30%	Stbd Tens 50%	Port Tens 50%
Wave Induced Torsional Moment	0.0	0.0	0.0	0.0	(-) 60%	(+) 60%	(-) 100%	(+) 100%
Wave Heading Angle	Head & Follow	Head & Follow	Head & Follow	Head & Follow	Beam	Beam	Oblique	Oblique

Notes:

- 1 Wave induced vertical bending moment is defined in 3-2-1/3.5 of the *Steel Vessel Rules*.
- 2 Wave induced horizontal bending moment is defined in 5C-3-3/5.3.1 of the *Steel Vessel Rules*.
- 3 Wave induced torsional moment and sign convention are defined in 5C-3-3/5.3.3 of the *Steel Vessel Rules*.

4.3.1 Standard Load Combination Cases

4.3.1(a) Calculate dynamic component of stresses for load cases LC1 through LC8, respectively.

4.3.1(b) Calculate four sets of stress ranges, one each for the following four pairs of combined loading cases.

LC1 and LC2,

LC3 and LC4,

LC5 and LC6, and

LC7 and LC8

4.3.2 Vessels with Either Special Loading Patterns or Special Structural Configuration

For vessels with either special loading patterns or special structural configurations/features, additional load cases may be required for determining the stress range.

5 Determination of Wave-induced Stress Range

5.1 General

This Subsection contains information on the fatigue inducing stress range to be used in the fatigue assessment.

Where, for a particular example shown, no specific value of SCF is given when one is called for, it indicates that a finite element analysis is needed. When the fine mesh finite element approach is used, additional information on calculations of stress concentration factors and the selection of compatible S-N data is given in Subsection A1/6.

5.2 Hatch Corners

5.2.1 Hatch Corners at Decks and Coaming Top (1 June 2017)

The peak stress range, f_R , for hatch corners at the strength deck, the top of the continuous hatch side coaming, and the lower decks which are effective for the hull girder strength may be approximated by the following equation:

$$f_R = 0.5^{1/\gamma} \times c_f (K_{s1} c_{L1} f_{RG1} + K_{s2} c_{L2} f_{RG2}) \quad \text{N/cm}^2 \text{ (kgf/cm}^2, \text{ lbf/in}^2\text{)}$$

where

- f_{RG1} = global dynamic longitudinal stress range at the inboard edge of the strength deck, top of continuous hatch side coaming, and lower deck of hull girder section under consideration clear of hatch corner, in N/cm^2 (kgf/cm^2 , lbf/in^2)
- $$= |f_{d1vi} - f_{d1vj}| + |f_{d1hi} - f_{d1hj}| + |f_{d1wi} - f_{d1wj}|$$
- f_{RG2} = bending stress range in connection with hull girder twist induced by torsion in cross deck structure in the transverse direction, in N/cm^2 (kgf/cm^2 , lbf/in^2)
- $$= |f_{d1ci} - f_{d1cj}|$$
- c_f = adjustment factor to reflect a mean wasted condition
- $$= 1.05$$
- f_{d1vi}, f_{d1vj} = wave-induced component of the primary stresses produced by hull girder vertical bending, in N/cm^2 (kgf/cm^2 , lbf/in^2), for load case i and j of the selected pairs of combined load cases, respectively. See 5C-5-3/5.1.1 and 3-2-1/3.5 of the *Steel Vessel Rules*
- f_{d1hi}, f_{d1hj} = wave-induced component of the primary stresses produced by hull girder horizontal bending, in N/cm^2 (kgf/cm^2 , lbf/in^2), for load case i and j of the selected pairs of combined load cases, respectively. See 5C-5-3/5.1.3 and 5C-3-3/5.3.1 of the *Steel Vessel Rules*
- f_{d1wi}, f_{d1wj} = wave-induced component of the primary stresses produced by hull girder torsion (warping stress) moment, in N/cm^2 (kgf/cm^2 , lbf/in^2), for load case i and j of the selected pairs of combined load cases, respectively. See 5C-5-3/5.1.5 and 5C-3-3/5.3.3 of the *Steel Vessel Rules*.

For calculating the wave-induced stresses, sign convention is to be observed for the respective directions of wave-induced loads, as specified in Appendix 1, Tables 4 and 5. These wave-induced stresses are to be determined based on the gross ship scantlings (A1/1.4).

f_{d1v} and f_{d1h} may be calculated by a simple beam approach. f_{d1w} in way of hatch corners at strength deck, top of continuous hatch side coaming, and lower deck may be determined from the full ship finite element model.

γ is as defined in A1/3.3.

K_{s1} and K_{s2} are stress concentration factors for the hatch corners considered and can be obtained by a direct finite element analysis. When a direct analysis is not available, these may be obtained from the following equations, but are not to be taken less than 1.0:

$$K_{s1} = c_t \alpha_{t1} \alpha_c \alpha_s k_{s1}$$

$$K_{s2} = \alpha_{ct} \alpha_{t2} k_{s2}$$

where

k_{s1} = nominal stress concentration factor in longitudinal direction, as given in the table below

k_{s2} = nominal stress concentration factor in transverse direction, as given in the table below

c_t = 0.8 for locations where coaming top terminates
= 1.0 for other locations

α_c = adjustment factor for cutout at hatch corners

$$= 1.0 \quad \text{for shapes without cutout}$$

$$= [1 - 0.04(c/R)^{3/2}] \quad \text{for circular shapes with a cutout}$$

$$= [1 - 0.04(c/r_d)^{3/2}] \quad \text{for double curvature shapes with a cutout}$$

$$= [1 - 0.04(c/R_1)^{3/2}] \quad \text{for elliptical shapes with a cutout}$$

$$\begin{aligned} \alpha_s &= \text{adjustment factor for contour curvature} \\ &= 1.0 && \text{for circular shapes} \\ &= 0.33[1 + 2(r_{s1}/r_d) + 0.1(r_d/r_{s1})^2] && \text{for double curvature shapes} \\ &= 0.33[1 + 2(R_2/R_1) + 0.1(R_1/R_2)^2] && \text{for elliptical shapes} \\ \alpha_{ct} &= 1.0 && \text{for shapes without cutout} \\ &= 0.5 && \text{for shapes with cutout} \\ \alpha_{t1} &= (t_s/t_i)^{1/2} \\ \alpha_{t2} &= 6.0/[5.0 + (t_i/t_c)], \text{ but not less than } 0.85 \end{aligned}$$

α_{t1} or α_{t2} is to be taken as 1.0 where the longitudinal or transverse extent of the reinforced plate thickness in way of the hatch corner is less than that required in A1/5.2.3, as shown in Appendix 1, Figure 2.

$$\begin{aligned} r_{s1} &= R && \text{for circular shapes in Appendix 1, Figure 3, in mm (in.)} \\ &= [3R_1/(R_1 - R_2) + \cos \theta]r_{e2}/[3.816 + 2.879R_2/(R_1 - R_2)] && \text{for double curvature shapes in Appendix 1, Figure 4, in mm (in.)} \\ &= R_2 && \text{for elliptical shapes in Appendix 1, Figure 5, in mm (in.)} \\ r_{s2} &= R && \text{for circular shapes in Appendix 1, Figure 3, in mm (in.)} \\ &= R_2 && \text{for double curvature shapes in Appendix 1, Figure 4, in mm (in.)} \\ &= R_2^2/R_1 && \text{for elliptical shapes in Appendix 1, Figure 5, in mm (in.)} \\ r_d &= (0.753 - 0.72R_2/R_1)[R_1/(R_1 - R_2) + \cos \theta]r_{e1} \\ t_s &= \text{plate thickness of the strength deck, hatch side coaming top, or lower deck} \\ & \quad \text{clear of the hatch corner under consideration, in mm (in.)} \\ t_c &= \text{plate thickness of the cross deck, hatch end coaming top, or bottom of cross} \\ & \quad \text{box beam clear of the hatch corner under consideration, in mm (in.)} \\ t_i &= \text{plate thickness of the strength deck, hatch coaming top, or lower deck in way} \\ & \quad \text{of the hatch corner under consideration, in mm (in.)} \end{aligned}$$

R , R_1 , and R_2 for each shape are as shown in Appendix 1, Figures 3, 4 and 5.

θ for double curvature shapes is defined in Appendix 1, Figure 4.

r_{e1} and r_{e2} are also defined for double curvature shapes in A1/5.2.3.

$$\begin{aligned} r_{e1} &= R && \text{for circular shapes in Appendix 1, Figure 3, in mm (in.)} \\ &= R_2 + (R_1 - R_2)\cos \theta && \text{for double curvature shapes in Appendix 1, Figure 4, in} \\ & \quad \text{mm (in.)} \\ &= (R_1 + R_2)/2 && \text{for elliptical shapes in Appendix 1, Figure 5, in mm (in.)} \\ r_{e2} &= R && \text{for circular shapes in Appendix 1, Figure 3, in mm (in.)} \\ &= R_1 - (R_1 - R_2)\sin \theta && \text{for double curvature shapes in Appendix 1, Figure 4, in} \\ & \quad \text{mm (in.)} \\ &= R_2 && \text{for elliptical shapes in Appendix 1, Figure 5, in mm (in.)} \end{aligned}$$

k_{s1}

r_{s1}/w_1	0.1	0.2	0.3	0.4	0.5
k_{s1}	1.945	1.89	1.835	1.78	1.725

k_{s2}

r_{s2}/w_2	0.1	0.2	0.3	0.4	0.5
k_{s2}	2.35	2.20	2.05	1.90	1.75

Note: k_{s1} and k_{s2} may be obtained by interpolation for intermediate values of r_{s1}/w_1 or r_{s2}/w_2 .

where

- w_1 = width of the cross deck under consideration, in mm (in.), for hatch corners of the strength deck and lower deck
= $0.1b_1$ for width of cross deck that is not constant along hatch length
- w_2 = width of the cross deck under consideration, in mm (in.), for strength deck and lower deck
- b_1 = width of the hatch opening under consideration, in mm (in.)

K_{s1} and K_{s2} for hatch corners with configurations other than those specified in this Appendix are to be determined from fine mesh finite element analysis.

The angle, ϕ , in degrees, along the hatch corner contour is defined as shown in Appendix 1, Figures 3, 4, and 5, and c_{L1} and c_{L2} at a given ϕ may be obtained by the following equations. For determining the maximum f_R , c_{L1} and c_{L2} are to be calculated at least for 5 locations (i.e., at $\phi = \phi_1$, ϕ_2 and three intermediate angles for each pair of the combined load cases considered).

- For circular shapes, $25 \leq \phi \leq 55$

$$c_{L1} = 1 - 0.00045(\phi - 25)^2$$

$$c_{L2} = 0.8 - 0.0004(\phi - 55)^2$$

- For double curvature shapes, $\phi_1 \leq \phi \leq \phi_2$

$$c_{L1} = [1.0 - 0.02(\phi - \phi_1)]/[1 - 0.015(\phi - \phi_1) + 0.00014(\phi - \phi_1)^2] \text{ for } \theta < 55$$

$$= [1.0 - 0.026(\phi - \phi_1)]/[1 - 0.03(\phi - \phi_1) + 0.0012(\phi - \phi_1)^2] \text{ for } \theta \geq 55$$

$$c_{L2} = 0.8/[1.1 + 0.035(\phi - \phi_2) + 0.003(\phi - \phi_2)^2]$$

where

$$\phi_1 = \mu(95 - 70r_{s1}/r_d)$$

$$\phi_2 = 95/(0.6 + r_{s1}/r_d)$$

$$\mu = 0.165(\theta - 25)^{1/2} \quad \text{for } \theta < 55$$

$$= 1.0 \quad \text{for } \theta \geq 55$$

- For elliptical shapes, $\phi_1 \leq \phi \leq \phi_2$

$$c_{L1} = 1 - 0.00004(\phi - \phi_1)^3$$

$$c_{L2} = 0.8/[1 + 0.0036(\phi - \phi_2)^2]$$

where

$$\phi_1 = 95 - 70R_2/R_1$$

$$\phi_2 = 88/(0.6 + R_2/R_1)$$

The peak stress range, f_R , is to be obtained through calculations of c_{L1} and c_{L2} at each ϕ along a hatch corner.

The formulas for double curvature shapes and elliptical shapes may be applicable to the following range:

$$0.3 \leq R_2/R_1 \leq 0.6 \text{ and } 45^\circ \leq \theta \leq 80^\circ \quad \text{for double curvature shapes}$$

For hatch coaming top and longitudinal deck girders, R_2/R_1 may be reduced to 0.15.

$$0.3 \leq R_2/R_1 \leq 0.9 \quad \text{for elliptical shapes}$$

5.2.2 Hatch Corners at the End Connections of Longitudinal Deck Girder

The total stress range, f_R , for hatch corners at the connection of longitudinal deck girder with cross deck box beam may be approximated by the following equation:

$$f_R = 0.5^{1/\gamma} \times c_f (\alpha_i K_{d1} f_{RG1} + K_{d2} f_{RG2}) \quad \text{N/cm}^2 \text{ (kgf/cm}^2, \text{ lbf/in}^2\text{)}$$

where

f_{RG1} = wave-induced stress range by hull girder vertical and horizontal bending moments and torsional moment at the longitudinal deck girder of hull girder section, in N/cm^2 (kgf/cm^2 , lbf/in^2)

$$= |f_{d1vi} - f_{d1vj}| + |f_{d1hi} - f_{d1hj}| + |f_{d1wi} - f_{d1wj}|$$

f_{RG2} = wave-induced stress range by hull girder torsional moment at the connection of the longitudinal deck girder with the cross deck box beam, in N/cm^2 (kgf/cm^2 , lbf/in^2)

$$= |f_{d1di} - f_{d1dj}|$$

α_i = 1.0 for symmetrical section of the longitudinal deck girder about its vertical neutral axis

= 1.25 for unsymmetrical section of the longitudinal deck girder about its vertical neutral axis

c_f and γ are as defined in A1/5.2.1 and A1/3.3.

f_{d1vi} , f_{d1vj} , f_{d1hi} , f_{d1hj} , f_{d1wi} , and f_{d1wj} are as defined in A1/5.2.1.

K_{d1} and K_{d2} may be obtained from the following equations, but not to be taken less than 1.0:

$$K_{d1} = 1.0$$

$$K_{d2} = \alpha_i \alpha_s k_d$$

where

k_d = nominal stress concentration factor as given in the table below

α_s = 1.0 for circular shapes

$$= 0.33[1 + 2(r_{s1}/r_d) + 0.1(r_d/r_{s1})^2] \quad \text{for double curvature shapes}$$

$$= 0.33[1 + 2(R_2/R_1) + 0.1(R_1/R_2)^2] \quad \text{for elliptical shapes}$$

$$\alpha_i = (t_d/t_i)^{1/2}$$

α_f is to be taken as 1.0 where longitudinal or transverse extent of the reinforced plate thickness in way of the hatch corner is less than that in A1/5.2.3, as shown in Appendix 1, Figure 6.

t_d = flange plate thickness of the longitudinal deck girder clear of the hatch corner under consideration, in mm (in.)

t_i = plate thickness at the end connection of the longitudinal deck girder under consideration, in mm (in.).

R , R_1 and R_2 for each shape are as shown in Appendix 1, Figures 3, 4 and 5.

θ for double curvature shapes is defined in Appendix 1, Figure 4.

r_{s1} and r_d are as defined for double curvature shapes in A1/5.2.1, above.

r_{e1} and r_{e2} are as defined for double curvature shapes in A1/5.2.3, below.

k_d

r_{s1}/w_d	0.1	0.2	0.3	0.4	0.5
k_d	2.35	2.20	2.05	1.90	1.75

Note: k_d may be obtained by interpolation for intermediate values of r_{s1}/w_d .

where

w_d = width of the longitudinal deck girder, in mm (in.)

5.2.3 Extent of Reinforced Plate Thickness at Hatch Corners

Where plating of increased thickness is inserted at hatch corners, the extent of the inserted plate, as shown in Appendix 1, Figures 2 and 6, is to be generally not less than that obtained from the following:

$$\ell_i = 1.75r_{e1} \quad \text{mm (in.)}$$

$$b_i = 1.75r_{e2} \quad \text{mm (in.)}$$

$$b_d = 1.1r_{e2} \quad \text{mm (in.)}$$

For a cut-out radius type:

$$\ell_{i1} = 1.75r_{e1} \quad \text{mm (in.)}$$

$$\ell_{i2} = 1.0r_{e1} \quad \text{mm (in.)}$$

$$b_i = 2.5r_{e2} \quad \text{mm (in.)}$$

$$b_d = 1.25r_{e2} \quad \text{mm (in.)}$$

where

r_{e1}	$= R$	for circular shapes in Appendix 1, Figure 3, in mm (in.)
	$= R_2 + (R_1 - R_2)\cos \theta$	for double curvature shapes in Appendix 1, Figure 4, in mm (in.)
	$= (R_1 + R_2)/2$	for elliptical shapes in Appendix 1, Figure 5, in mm (in.)
r_{e2}	$= R$	for circular shapes in Appendix 1, Figure 3, in mm (in.)
	$= R_1 - (R_1 - R_2)\sin \theta$	for double curvature shapes in Appendix 1, Figure 4, in mm (in.)
	$= R_2$	for elliptical shapes in Appendix 1, Figure 5, in mm (in.)

At welding joints of the inserted plates to the adjacent plates, a suitable transition taper is to be provided and the fatigue assessment at these joints may be approximated by the following:

$$f_R = 0.5^{1/\gamma} \times c_f K_t f_s \quad \text{N/cm}^2 \text{ (kgf/cm}^2, \text{ lbf/in}^2\text{)}$$

where

$$\begin{aligned} f_s &= \text{nominal stress range at the joint under consideration} \\ &= f_{RG1} \quad \text{for side longitudinal deck box, as specified in A1/5.2.1, in} \\ & \quad \text{N/cm}^2 \text{ (kgf/cm}^2, \text{ lbf/in}^2\text{)} \\ &= f_{RG2} \quad \text{for cross deck box beam, as specified in A1/5.2.1, in N/cm}^2 \\ & \quad \text{(kgf/cm}^2, \text{ lbf/in}^2\text{)} \\ &= f_{RG1} + f_{RG2} \quad \text{for longitudinal deck girder, as specified in A1/5.2.2, in N/cm}^2 \\ & \quad \text{(kgf/cm}^2, \text{ lbf/in}^2\text{)} \\ K_t &= 0.25(1 + 3t_i/t_a) \leq 1.25 \\ t_i &= \text{plate thickness of inserted plate, in mm (in.)} \\ t_a &= \text{plate thickness of plate adjacent to the inserted plate, in mm (in.)} \end{aligned}$$

c_f and γ are as defined in A1/5.2.1 and A1/3.3.

FIGURE 2
Hatch Corners at Decks and Coaming Top

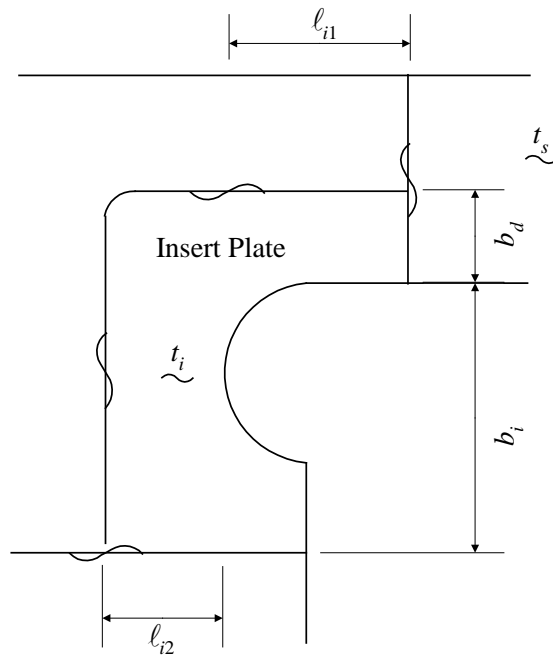
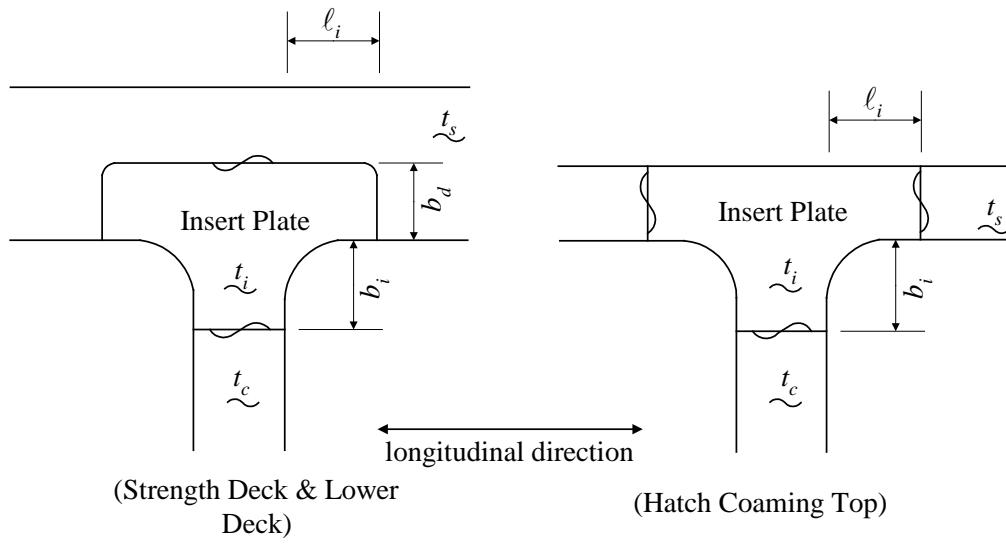


**FIGURE 3
Circular Shape**

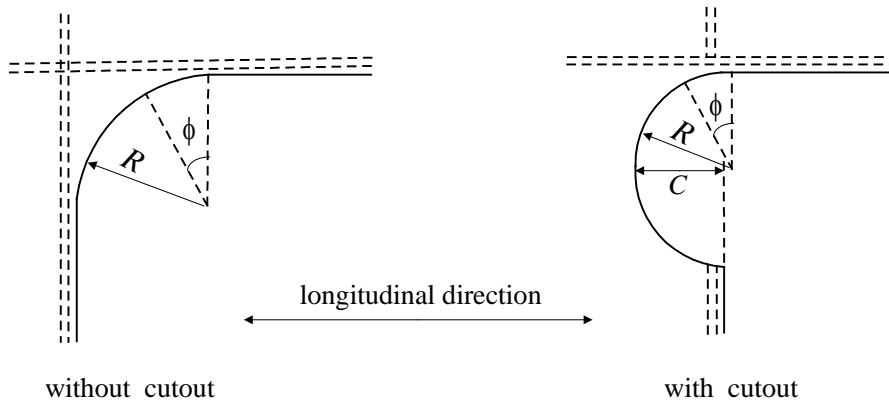


**FIGURE 4
Double Curvature Shape**

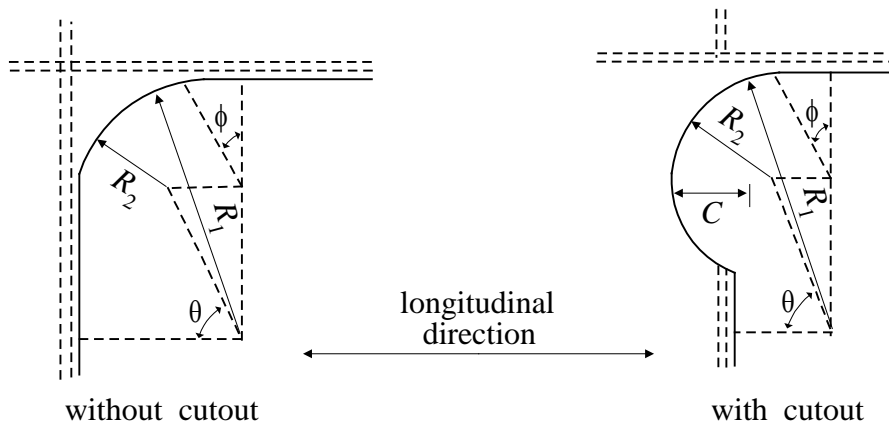


**FIGURE 5
Elliptical Shape**

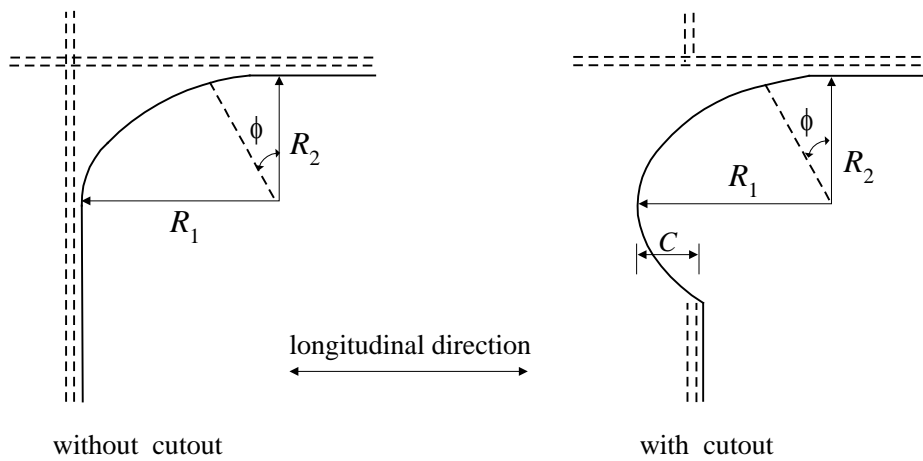
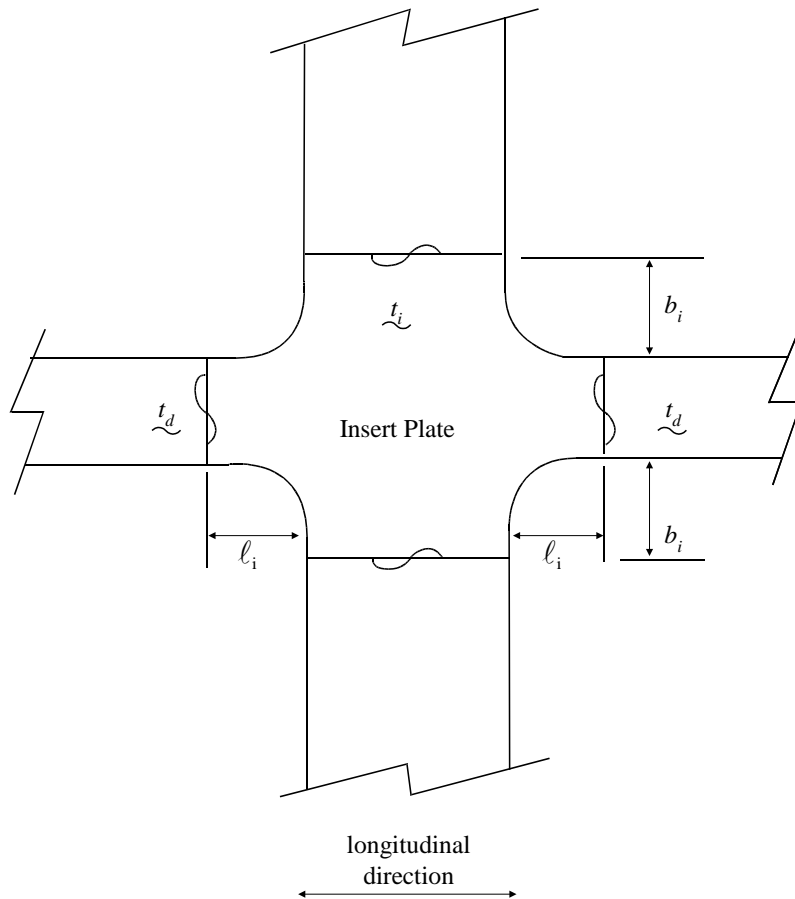


FIGURE 6
Hatch Corner for Longitudinal Deck Girder



6 Hot Spot Stress Approach with Finite Element Analysis

6.1 Introduction

In principle, the fatigue strength of all connections can be assessed with the hot spot stress approach described in this Subsection. However, for some details as indicated in A1/2.2, in lieu of the hot spot stress approach, the nominal stress approach can also be employed to evaluate the fatigue strength.

Hot spot stress is defined as the surface stress at the hot spot. Note that the stress change caused by the weld profile is not included in the hot spot stress, but the overall effect of the connection geometry on the nominal stress is represented. Therefore, in hot spot stress approach, the selection of an S-N curve depends on: 1) weld profile, i.e., existence of weld and weld type (fillet, partial penetration or full penetration); 2) predominant direction of principal stress; and 3) crack locations (toe, root or weld throat).

There are various adjustments (reductions in capacity) that may be required to account for factors such as a lack of corrosion protection (coating) of structural steel and relatively large plate thickness. The imposition of these adjustments on fatigue capacity will be in accordance with ABS practice for vessels.

There are other adjustments that could be considered to increase fatigue capacity above that portrayed by the cited S-N data. These include adjustments for compressive “mean stress” effects, a high compressive portion of the acting variable stress range, and the use of “weld improvement” techniques. The use of a weld improvement technique, such as weld toe grinding or peening to relieve ambient residual stress, can be effective in increasing fatigue life. However, credit should not be taken of such a weld improvement in the design phase of the structure. Consideration for granting credit for the use of weld improvement techniques is to be reserved for situations arising during construction, operation, or future reconditioning of the structure.

An exception may be made if the target design fatigue life cannot be satisfied by other preferred design measures such as refining layout, geometry, scantlings, and welding profile to minimize fatigue damage due to high stress concentrations. Grinding or ultrasonic peening can be used to improve fatigue life in such cases. The calculated fatigue life is to be greater than 15 years excluding the effects of life improvement techniques. Where improvement techniques are applied, full details of the improvement technique standard including the extent, profile smoothness particulars, final weld profile, and improvement technique workmanship and quality acceptance criteria are to be clearly shown on the applicable drawings and submitted for review together with supporting calculations indicating the proposed factor on the calculated fatigue life.

Grinding is preferably to be carried out by rotary burr and to extend below the plate surface in order to remove toe defects, and the ground area is to have effective corrosion protection. The treatment is to produce a smooth concave profile at the weld toe with the depth of the depression penetrating into the plate surface to at least 0.5 mm below the bottom of any visible undercut. The depth of groove produced is to be kept to a minimum, and, in general, kept to a maximum of 1 mm. In no circumstances is the grinding depth to exceed 2 mm or 7% of the plate gross thickness, whichever is smaller. Grinding is to extend to areas well outside the highest stress region.

The finished shape of a weld surface treated by ultrasonic peening is to be smooth, and all traces of the weld toe are to be removed. Peening depths below the original surface are to be maintained to at least 0.2 mm. Maximum depth is generally not to exceed 0.5 mm.

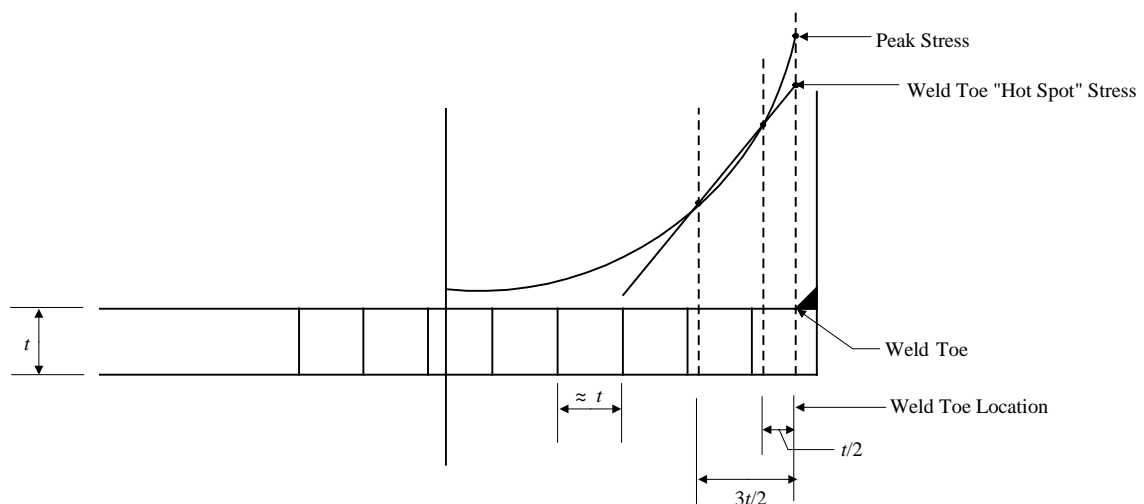
Provided these recommendations are followed, an improvement in fatigue life by grinding or ultrasonic peening up to a maximum of 2 times may be granted.

6.2 Calculation of Hot Spot Stress at a Weld Toe

Appendix 1, Figure 7 shows an acceptable method which can be used to extract and interpret the “near weld toe” element dynamic stress ranges (referred to as stresses for convenience in the following text in this Subsection) and to obtain a (linearly) extrapolated stress (dynamic stress range) at the weld toe. When plate or shell elements are used in the modeling, it is recommended that each element size is to be equal to the plate thickness.

Weld hot spot stress can be determined from linear extrapolation of surface component stresses at $t/2$ and $3t/2$ from weld toe. The principal stresses at hot spot are then calculated based on the extrapolated stresses and used for fatigue evaluation. Description of the numerical procedure is given below.

FIGURE 7



The algorithm described in the following is applicable to obtain the hot spot stress for the point at the toe of a weld. The weld typically connects either a flat bar member or a bracket to the flange of a longitudinal stiffener, as shown in Appendix 1, Figure 8.

Consider the four points, P_1 to P_4 , measured by the distances X_1 to X_4 from the weld toe, designated as the origin of the coordinate system. These points are the centroids of four neighboring finite elements, the first of which is adjacent to the weld toe. Assuming that the applicable surface component stresses (or dynamic stress ranges), S_i , at P_i have been determined from FEM analysis, the corresponding stresses at “hot spot” (i.e., the stress at the weld toe) can be determined by the following procedure:

6.2.1

Select two points, L and R , such that points L and R are situated at distances $t/2$ and $3t/2$ from the weld toe; i.e.:

$$X_L = t/2, \quad X_R = 3t/2$$

where t denotes the thickness of the member to which elements 1 to 4 belong (e.g., the flange of a longitudinal stiffener).

6.2.2

Let $X = X_L$ and compute the values of four coefficients, as follows:

$$C_1 = [(X - X_2)(X - X_3)(X - X_4)] / [(X_1 - X_2)(X_1 - X_3)(X_1 - X_4)]$$

$$C_2 = [(X - X_1)(X - X_3)(X - X_4)] / [(X_2 - X_1)(X_2 - X_3)(X_2 - X_4)]$$

$$C_3 = [(X - X_1)(X - X_2)(X - X_4)] / [(X_3 - X_1)(X_3 - X_2)(X_3 - X_4)]$$

$$C_4 = [(X - X_1)(X - X_2)(X - X_3)] / [(X_4 - X_1)(X_4 - X_2)(X_4 - X_3)]$$

The corresponding stress at Point L can be obtained by interpolation as:

$$S_L = C_1 S_1 + C_2 S_2 + C_3 S_3 + C_4 S_4$$

6.2.3

Let $X = X_R$ and repeat the step in A1/6.2.2 to determine four new coefficients. The stress at Point R can be interpolated likewise, i.e.:

$$S_R = C_1 S_1 + C_2 S_2 + C_3 S_3 + C_4 S_4$$

6.2.4

The corresponding stress at hot spot, S_0 , is given by

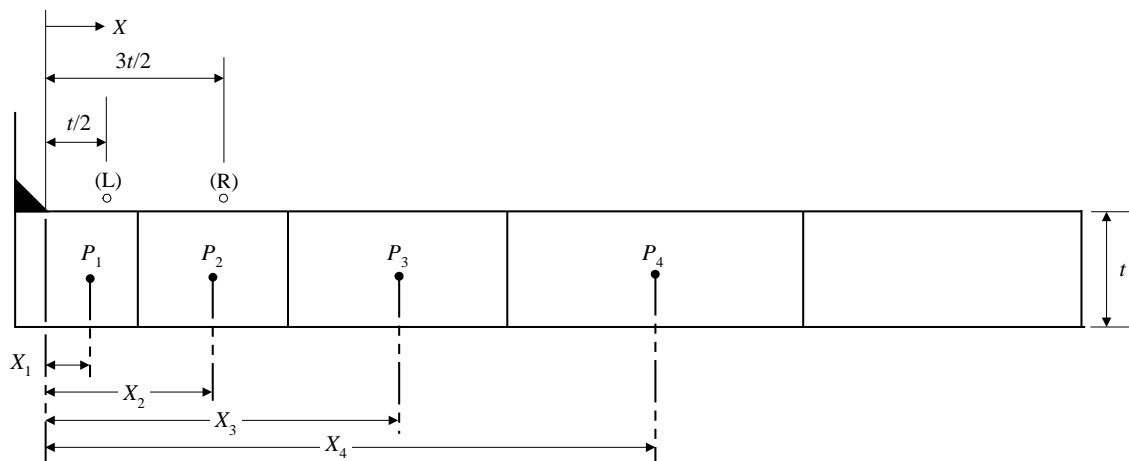
$$S_0 = (3S_L - S_R)/2$$

Notes:

The algorithm presented in the foregoing involves two types of operations. The first is to utilize the stress values at the centroid of the four elements considered to obtain estimates of stress at Points L and R by way of an interpolation algorithm known as Lagrange interpolation. The second operation is to make use of the stress estimates, S_L and S_R , to obtain the hot spot stress via linear extrapolation.

While the Lagrange interpolation is applicable to any order of polynomial, it is not advisable to go beyond the 3rd order (cubic). Also, the even order polynomials are biased, so that leaves the choice between a linear scheme and a cubic scheme. Therefore, the cubic interpolation, as described in A2/6.2.2, should be used. It can be observed that the coefficients, C_1 to C_4 are all cubic polynomials. It is also evident that, when $X = X_j$, which is not equal to X_i , all of the C 's vanish except C_i , and if $X = X_i$, $C_i = 1$.

FIGURE 8



6.3 Calculation of Hot Spot Stress at the Edge of Cut-out or Bracket

In order to determine the hot spot stress at the edge of cut-out or bracket, dummy rod elements can be attached to the edge. The sectional area of the dummy rod may be set at 0.01 cm^2 . The mesh needs to be fine enough to determine the local stress concentration due to the geometry change. The axial stress range of the dummy rod is to be used to assess the fatigue strength of the cut-out or bracket (edge crack).